PhotoniX

REVIEW Open Access

Artificial intelligence-driven distributed acoustic sensing technology and engineering application

Liyang Shao[1*], Jingming Zhang[1,2], Xingwei Chen[1], Deyu Xu[1], Huaxin Gu[1], Qi Mu[1], Feihong Yu[1], Shuaiqi Liu[1], Xiaobing Shi[1], Jiayao Sun[1], Zixing Huang[1], Xiongji Yang[1], Haifeng Zhang[1,3], Yunbin Ma[4], Han Lu[5], Chuanqing Liu[5] and Changyuan Yu[2]

Jingming Zhang co-first author.

*Correspondence: shaoly@sustech.edu.cn

[1] Department of Electrical and Electronic Engineering, Southern University of Science and Technology, Shenzhen, Guangdong, China
[2] Department of Electrical and Electronic Engineering, The Hong Kong Polytechnic University, Hong Kong (SAR), China
[3] Energy Advanced Measurement and Control and Equipment R&D Center, Research Institute of Tsinghua University, Pearl River Delta, Guangzhou, Guangdong, China
[4] PipeChina Institute of Science and Technology, Langfang, Hebei, China
[5] Shenzhen Gas Corporation Ltd, Shenzhen, Guangdong, China

Abstract

Distributed acoustic sensing (DAS) technology is a fiber-optic based distributed sensing technology. It achieves real-time monitoring of acoustic signals by detecting weak disturbances along the fiber. It has advantages such as long measurement distance, high spatial resolution and large dynamic range. Artificial intelligence (AI) has great application potential in DAS technology, including data augmentation, preprocessing and classification and recognition of acoustic events. By introducing AI algorithms, DAS system can process massive data more automatically and intelligently. Through data analysis and prediction, AI-enabled DAS technology has wide applications in fields such as transportation, energy and security due to its accuracy of monitoring data and reliability of intelligent decision-making. In the future, the continuous advancement of AI technology will bring greater breakthroughs and innovations for the engineering application of DAS technology, play a more important role in various fields, and promote the innovation and development of the industry.

Keywords: Distributed acoustic sensing (DAS), Artificial intelligence (AI), Engineering application

Introduction

Distributed acoustic sensing (DAS) is an emerging sensing technology that has received widespread attention and research in recent years. Unlike traditional point sensors, DAS uses optical fibers as sensors to sense and analyze sound signals in the environment in real-time and with high precision, thereby obtaining information on the propagation of sound waves and events in the environment.

In recent years, the rapid development of artificial intelligence (AI) technology has attracted widespread attention and research. AI has shown remarkable potential and application prospects in various fields, especially in natural language processing and computer vision, achieving significant breakthroughs. The combination of traditional DAS technology and AI technology can achieve fast and accurate processing and analysis of sound signals through intelligent algorithms and system design. AI-driven DAS

technology mainly includes four stages: data acquisition, preprocessing, feature extraction, and machine learning model construction. Data is the foundation of machine learning, and the DAS field faces problems such as difficulty in data acquisition and large data volume, which to some extent limits the development of machine learning. To overcome these problems, establishing public DAS datasets for various scenarios can effectively reduce the difficulty of data acquisition and provide a fair comparison and evaluation platform for different models [1–4]. In addition, research on data augmentation methods [1, 5] can improve the robustness and generalization ability of models, providing new solutions for the recognition of small-sample events. Furthermore, data compression algorithms [6] can significantly reduce data volume while retaining effective information, reducing the cost of data collection and storage. Data preprocessing usually includes two steps: denoising and feature extraction. Denoising algorithms can effectively reduce the impact of Gaussian noise, phase noise, and fading on signals. Common denoising algorithms include filtering [7–9], decomposition [10–13], image-based denoising algorithms [14–18], and deep learning methods [19, 20]. For feature extraction, appropriate feature selection can improve the accuracy of classification models. Time–frequency images [21], Mel cepstrum [1], and wavelet transforms [22] are commonly used statistical features in traditional machine learning. At the same time, mapping methods from time series to two-dimensional images, such as short-time Fourier transform [23, 24] and Gramian Angular Field (GAF) [25, 26], provide feature images for deep learning. In terms of machine learning model construction, traditional machine learning methods include support vector machines (SVM) [7, 21, 27], hidden Markov models (HMM) [28–30], etc. Deep learning models based on convolutional neural networks (CNN) [25, 26, 31] have gradually become the mainstream algorithm for DAS pattern recognition due to their advantages in computer vision.

DAS technology has a wide range of applications and has shown unique advantages in various fields such as transportation [32–34], energy [35–42], and security [43–47] by monitoring and analyzing sound signals in the environment in real-time. In the transportation field, DAS technology can be used for road monitoring and intelligent transportation systems. By using distributed optical fiber sensors, it can monitor the vibration and deformation of roads in real-time, detect the health status of road structures in a timely manner, and warn of potential problems such as cracks and subsidence. Additionally, DAS technology can also be used in intelligent transportation systems to help optimize traffic signal control, traffic flow management, and congestion prediction, thereby improving traffic efficiency and safety. In the energy field, DAS technology can be used for oil and gas pipeline monitoring and power system monitoring. Oil and gas pipelines are important channels for energy transportation. Through DAS technology, pipeline vibration, temperature, and leakage can be monitored in real-time, and potential problems can be detected and handled in a timely manner to ensure the safety and stable operation of pipelines. In the power system, DAS technology can be used to monitor the status of transmission lines and substations, identify the health status of lines, power loads, and short-circuit faults in real-time, and help improve the reliability and safety of the power grid. In the perimeter security field, DAS technology is widely used in boundary and fence monitoring. By installing optical fiber sensors in the fence, DAS technology can detect whether the fence is damaged or whether intruders are approaching in

real-time, and issue timely alarms and take measures. Additionally, DAS technology can also be used to monitor the vibration and sound signals of the perimeter, providing early warning and protection for important facilities and places. With the further development of technology, the application prospects of DAS technology will continue to expand.

In this paper, we will comprehensively introduce the latest progress of AI-driven DAS technology and its applications, as shown in Fig. 1. First, we will describe in detail the working principle of the DAS system, including the intensity demodulation and phase demodulation schemes. In AI-driven DAS technology, we review and discussed the dataset, data preprocessing, and classification model in the AI process. Then, we review the application of DAS technology in engineering fields such as traffic monitoring, geological energy exploration, and security. Finally, we propose conclusions on AI-driven DAS technology research and prospects for its future development.

Principles of the DAS system

Theoretical model of Φ-OTDR

The DAS system utilizes the Rayleigh backscattered (RBS) [48–50], which has the highest scattering power in optical fibers, for real-time monitoring of individual physical quantities on the fiber. Compared to the traditional optical time-domain reflectometry (OTDR), the DAS system is based on a phase-sensitive optical time-domain reflectometry (Φ-OTDR), which utilizes a low-frequency-drift, narrow-linewidth laser as a high-coherence light source. During the propagation of a probe pulse, the scattered light within the pulse interferes, and the detected signal is a coherent superposition of the RBS signals within the pulse width.

To facilitate the explanation of the working principle of the DAS system, researchers have established a one-dimensional RBS signal model [51], as shown in Fig. 2. In this model, the optical fiber can be regarded as composed of countless cylindrical thin slices, and each

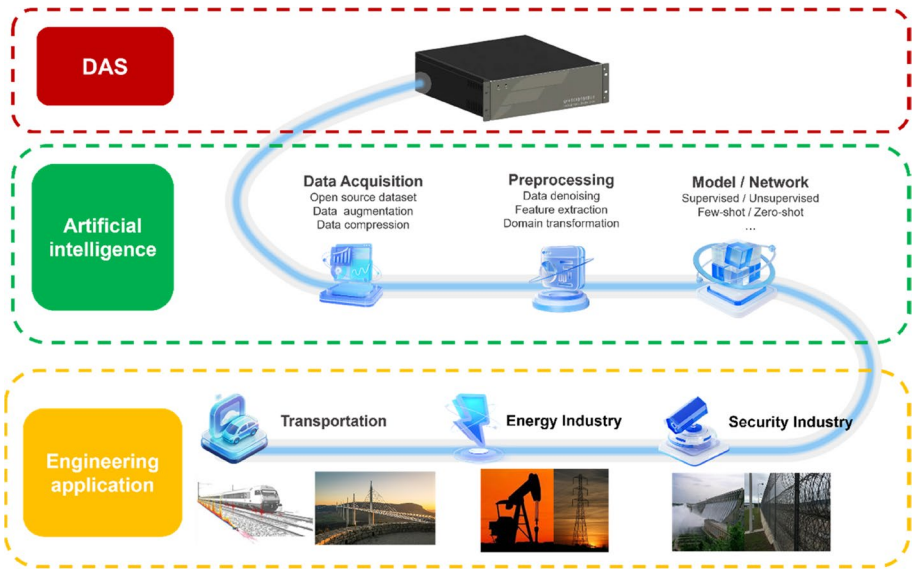

Fig. 1 AI-driven DAS technology and engineering application

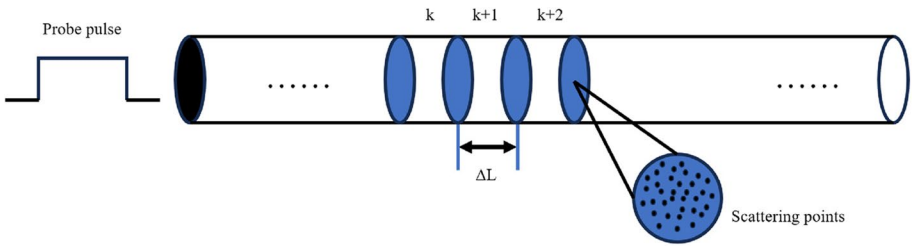

Fig. 2 One dimensional RBS signal model

cylindrical thin slice consists of a number of scattering points, assuming that there are a total of K cylindrical thin slices in the optical fiber of length L, and therefore the length of each cylindrical thin slice is $\Delta L = L/K$. The scattering signals generated by all the scattering points in each cylindrical thin slice are superimposed to form the scattering signal generated by the cylindrical thin slice.

Assuming that there are n scattering points within the kth cylindrical thin slice, the RBS signal generated by this cylindrical thin slice can be expressed by:

$$r_k = \sum_{i=1}^{n} a_i \exp(j\theta_i) = |r_k| \exp(j\varphi_k) \tag{1}$$

where θ_i and a_i denote the phase and intensity of a single scattering point, respectively. φ_k and $|r_k|$ denote the synthesized phase and synthesized intensity of the kth cylindrical thin slice, respectively. Since the length of each cylindrical thin slice is very small, the formula ignores the attenuation between different scattering points, and according to the knowledge of probability theory, it can be obtained that the intensity and the phase of each cylindrical thin slice obeys the Rayleigh distribution and the uniform distribution, respectively.

The expression for the RBS light generated at position z in the fiber is given by:

$$E_{RBS}(z) = E_0 \exp(-\alpha z) \exp(j2 \int_0^z f(x)dx) \sum_{k=1}^{M} r_k \exp(j2 \int_z^{z+M\Delta L} f(x)dx) \tag{2}$$

where E_0 is the amplitude of the probe pulse, α is the fiber attenuation coefficient, $f(x)$ is the optical transmission function, and M is the number of cylindrical thin slices contained within the pulse width. From Eq. (2), the amplitude and transmission phase of the Rayleigh-scattered synthesized light can be respectively expressed as

$$A_R(z) \exp[j\phi_R(z)] = \sum_{k=1}^{M} r_k \exp(j2 \int_z^{z+M\Delta L} f(x)dx) \tag{3}$$

$$\phi_T(z) = \int_0^z f(x)dx \tag{4}$$

where $\phi_R(z)$ is the phase of Rayleigh scattering synthesized light. From Eq. (4), the transmitted phase is linearly related to the external perturbation. Then Eq. (2) can be expressed as

$$\begin{aligned} E_{RBS}(z) &= E_0 A_R(z) \exp(-\alpha z) \exp[j2\phi_T(z) + j\phi_R(z)] \\ &= A_s(z) \exp[j\phi_s(z)] \end{aligned} \tag{5}$$

where $A_s(z)$ and $\phi_s(z)$ are the amplitude and phase of the received signal, respectively. From Eq. (5), if the perturbation occurs only at position z, the intensity and phase of the scattering signal generated at position z change, the scattering signal generated before position z do not change in intensity and phase because it occurs before the perturbation. The intensity of the scattered signal generated after position z remains unchanged and the synthesized phase $\phi_R(z)$ also remains unchanged. However, the transmission phase $\phi_T(z)$ is linearly correlated with the perturbation, and the optical phase at z and all positions thereafter is affected by the external perturbation.

Detection and demodulation scheme for DAS systems

From the principle of the DAS system, both the intensity and the phase of the scattered light can be modulated by perturbations. Therefore, the detection scheme aims at obtaining these two parameters.

Direct detection

The direct detection DAS system structure is shown in Fig. 3(a) [52]. The system uses an electro-optical modulator (EOM) to generate the probe pulse, and the intensity information of the scattered light can be obtained after the RBS light signal enters the photodetector (PD). The output electrical signal of the PD can be expressed as

$$I_{RBS}(t) = \xi \left| E_{RBS}(t) \cdot E_{RBS}(t)^* \right| = \xi A_s(t)^2 = \xi P_s(t) \tag{6}$$

where ξ is the response coefficient of the PD. From Eq. (6), the higher the scattered light power the larger the value of the PD output electrical signal. After obtaining the PD

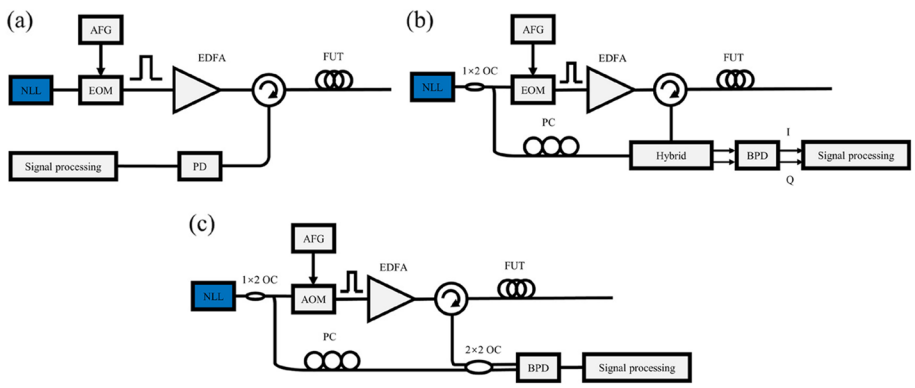

Fig. 3 **a** The setup of DAS system based on direct detection. **b** The setup of DAS system based on homodyne detection. **c** The setup of DAS system based on heterodyne detection (NLL: Narrow Linewidth Laser; AFG: Arbitrary Function Generator; EOM: Electrical Optical Modulator; AOM: Acoustic Optical Modulator; EDFA: Erbium Doped Fiber Amplifier; PD: Photo-Detector; PC: Polarization Controller; BPD: Balanced photodetector; FUT: Fiber Under Test; OC: Optical Coupler)

output signal strength, the exact perturbation position can be obtained by making a difference between neighboring RBS curves.

Coherence detection

Since there is no correspondence between the signal strength and the external perturbation, accurate perturbation information cannot be obtained from the direct detection DAS system. On the contrary, because the coherent detection DAS system can phase demodulate the scattered signal, the quantitative analysis of the perturbation can be realized. There are two main types of coherent detection: zero-difference coherent detection as well as out-of-phase coherent detection.

Homodyne detection The structure of the homodyne detection DAS system is shown in Fig. 3(b) [53]. The system uses the EOM to generate the probe pulse, and the 90° optical mixer (Hybrid) is used at the receiving end to generate a 90° phase shift for one of the RBS light signals, which then enters the balanced photodetector (BPD) for photoelectric conversion to generate the isochronous signal I and the quadrature signal Q. The system also uses a 90° optical mixer (Hybrid) to generate a 90° phase shift for the RBS light signals.

The electrical signal expression of the BPD output is given by

$$I_{RBS}(t) = \xi_1 A_s(t) A_{LO} \cos\theta(t) \cos[\phi(t)] \tag{7}$$

$$Q_{RBS}(t) = \xi_2 A_s(t) A_{LO} \cos\theta(t) \sin[\phi(t)] \tag{8}$$

where ξ_1 and ξ_2 are the response coefficients of the two BPDs, respectively. $\theta(t)$ and $\phi(t)$ are the relative polarization angle and relative phase angle between the scattered light and the reference light, respectively. If the response coefficients are the same, the final signal amplitude and phase obtained can be respectively expressed as

$$A(t) = \sqrt{I_{RBS}(t)^2 + Q_{RBS}(t)^2} = \xi A_s(t) A_{LO} \cos\theta(t) \tag{9}$$

$$\phi(t) = \arctan\left(\frac{Q_{RBS}(t)}{I_{RBS}(t)}\right) \tag{10}$$

Heterodyne detection The structure of the outlier detection DAS system is shown in Fig. 3(c) [54]. The system uses an acousto-optic modulator (AOM) to generate the probe pulse. The AOM has the function of frequency shifting. The expression for the AC component of the output electrical signal of the BPD is given by

$$I_{AC}(t) \propto 2\xi A_{LO} A_s(t) \cos\theta(t) \cos[\omega_A t + \phi(t)] \tag{11}$$

where ω_A is the frequency shift introduced by the AOM. $\theta(t)$ and $\phi(t)$ are the relative polarization angle and the relative phase angle between the scattered light and the local reference light, respectively. The complex signal of the original signal can be obtained by

the Hilbert transform, where $I_H = Hilbert(I_{AC}(t))$,and then the amplitude and phase of the signal can be obtained by I/Q demodulation as

$$A(t) = \sqrt{real[I_H(t)]^2 + imag[I_H(t)]^2} \tag{12}$$

$$\phi(t) = \arctan(\frac{imag[I_H(t)]}{real[I_H(t)]}) \tag{13}$$

AI-driven DAS technology

Machine learning is a branch of AI that studies how to improve performance by allowing computers to learn from experience, which is widely used in various fields. Due to the uncertainty of the sound source location and the complex noise environment, accurate pattern recognition of DAS data has always been a challenge. Machine learning is an effective method to solve this problem. By analyzing and modeling a large amount of DAS data, machine learning algorithms can automatically learn patterns and rules from the data, thereby achieving automatic classification and recognition of various sound patterns. Compared with traditional rule-based methods, Machine learning methods do not require prior knowledge of the field and can learn implicit relationships and patterns from data as judgment criteria. Machine learning methods can also improve the performance and robustness of DAS pattern recognition through feature selection and model optimization. However, machine learning methods still face some challenges in DAS pattern recognition, such as data imbalance and noise interference, which require further research. The workflow of AI-driven DAS technology includes data acquisition, preprocessing, feature extraction, and machine learning model.

Data acquisition

The core of machine learning is the use of large amounts of training data, and the quantity and quality of data directly affect the performance of the model. Compared with AI fields such as computer vision and audio recognition, DAS pattern recognition faces enormous challenges in terms of data. Obtaining DAS data requires complete experimental equipment, and in some scenarios, the deployment of optical fibers requires relevant permits. Additionally, equipment and server operation and maintenance costs may be required. Due to the lack of public DAS datasets, obtaining high-quality DAS data is still one of the problems faced by many researchers. Table 1 lists some open-source DAS datasets:

High-quality large-scale open-source datasets such as ImageNet can effectively promote the development of the machine learning field, enabling the comparison and evaluation of different models on a fair basis, and accurately assessing the value of these works. With the continuous development of DAS pattern recognition, the construction of open-source datasets applicable to different scenarios has become one of the urgent problems to be solved.

Data augmentation is another method to solve the difficulty of obtaining DAS data. Data augmentation is a method of expanding data. It can increase the number of samples in the training sets, effectively alleviate the problem of model overfitting, and bring

Table 1 Open-source DAS datasets

Project [Ref.]	Events	Year
Monitoring of hot spring geothermal Wells by DAS and DTS [3]	Acoustic, temperature changes and a seismic signal	2018
Submarine cable condition monitoring with DVS [55]	Abrupt impact and cyclical loading	2019
Railway track behavior analysis based on DAS [56]	Track deflection and load	2020
Different types of vibration events built using loudspeakers [1]	Mechanical activities, human activities and natural events	2021
Large open source DAS database from multiple experiments, mainly in the fields of seismology and geophysics [2]	It includes a variety of environments such as urban centers, underground mines and the seabed	2023
Simulation of DAS events in a laboratory environment [4]	Background noise, digging, knocking, shaking, watering and walking	2023

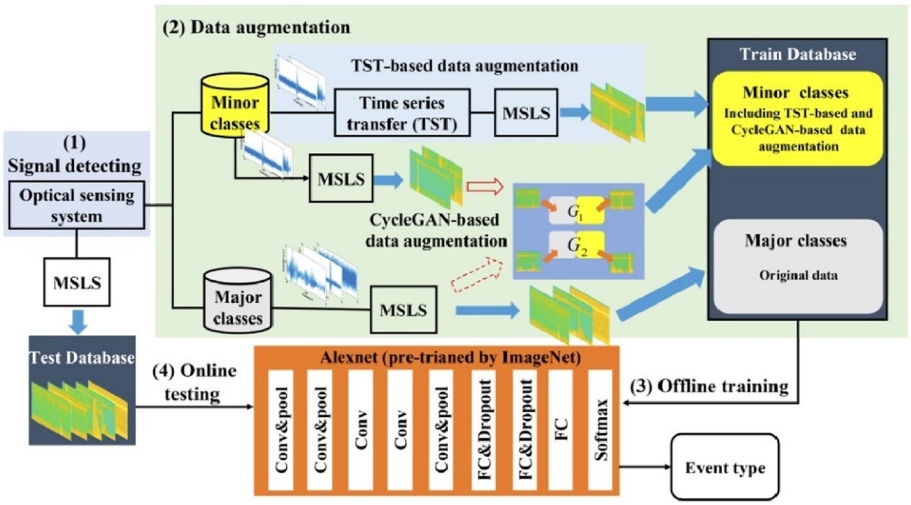

Fig. 4 Few-shot learning for DAS event recognition based on data augmentation (MSLS: Mel spectrum with log scale) [58]

stronger generalization ability to the model. Currently, research on DAS data augmentation is limited, mainly based on basic data augmentation. Researchers shift images to simulate changes in the location of events [5]; time stretching can change the frequency distribution of the original signal, which can provide more changes for each sample in a specific category [1]; image flipping, translation, brightness enhancement, cropping, and adding Gaussian noise are also commonly used data augmentation methods.

Generative adversarial networks (GANs) as a generative model have been attempted for DAS data generation. Researchers use GANs to refine computer-simulated data and train ANN classifiers. Compared with classifiers trained only with simulation data or experimental data, the network trained with GAN-generated data has significantly improved performance [57]. In 2022, researchers used data augmentation based on time-series transfer (TST) and cycle generative adversarial networks (CycleGAN) [58], which not only increased the amount of data but also improved the diversity of small-class data, as shown in Fig. 4. In the case where each of the two small classes contains only two samples, the average accuracy of the validation set of five classification tasks

can still reach 90.84%, and the classification accuracy of small classes can reach 79.28%, which is 44.45% higher than the basic augmentation method. However, the GAN model relies on a large amount of data for training. DAS data augmentation techniques based on deep learning still need further research. Shang et al. [59] proposed an innovative method combining k-SMOTE and deep convolutional generative adversarial network (DCGAN) for dual data augmentation, called kS-DCGAN. This method solves the problem of insufficient data samples of some types and increases the diversity of data. In addition, this paper uses the CycleGAN network to combine the normal sample characteristics collected by DAS with the fault sample characteristics collected by ordinary sensors to generate fault data that conform to the sample characteristics collected by DAS. This method can extend the number of fault samples from 0 to 1000.

DAS systems typically generate large amounts of data due to their high sampling rate, long distributed sensing distance, and small spatial resolution [60]. For example, in the field of geophysics, a DAS system with a sampling rate of 2000 Hz and a spatial resolution of 1 m for a sensing range of 2 km can produce approximately 650 GB of data per day [61]. High-density sampling generates massive amounts of data, which challenges existing data storage, management, and real-time processing systems. There is still considerable potential for improving computational efficiency. Data compression algorithms for DAS can significantly reduce data volume while retaining important information.

Currently, some data compression methods directly process demodulated signals [62, 63], effectively reducing data volume. Compression algorithms tailored to the characteristics of DAS systems [6, 64, 65] can fundamentally decrease data volume, further easing storage issues. However, these methods inevitably reduce the signal-to-noise ratio (SNR), necessitating a balance between data volume and system SNR. Our research team has proposed a hybrid compression method to reduce the data volume of heterodyne Φ-OTDR systems [66]. This method stores encoded spectral samples, which we refer to as the Spectral Extraction, Encoding, and Reconstruction (SEER) method, as illustrated in Fig. 5. Although this approach slightly increases computational load, it achieves a high compression ratio. Compared to storing time-domain waveforms, retaining encoded

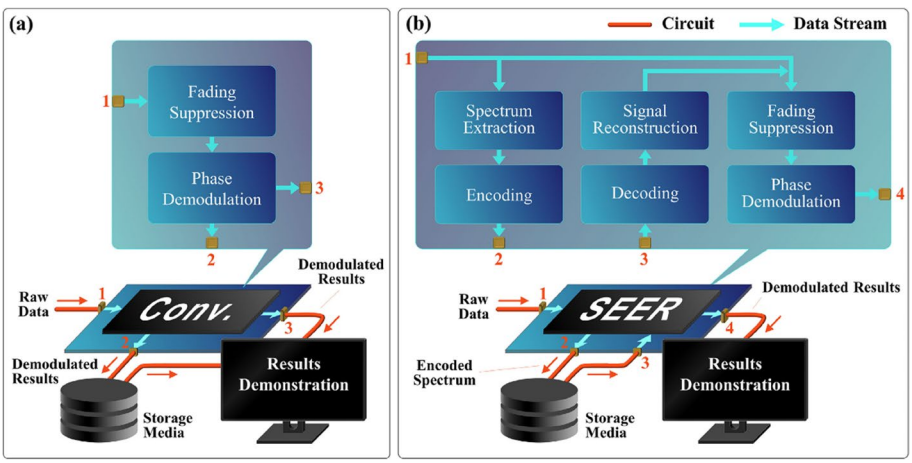

Fig. 5 Simplified data storage and results presentation process under (**a**) conventional approach and (**b**) SEER method [66]

spectral samples significantly reduces data volume. Additionally, this method preserves the dense sensing channel characteristics of the DAS system with minimal impact on other key system parameters. Furthermore, it allows simultaneous acquisition of phase and amplitude information, facilitating the extraction of multidimensional features in pattern recognition.

Data preprocessing

Data denoising and feature extraction are essential steps in building pattern recognition systems. The purpose of denoising is to reduce measurement noise and improve SNR. This task is crucial for long-distance DAS technology because as the sensing length increases, the sensing capability usually degrades to some extent. Denoising algorithms operate on raw data and output denoised data of the same dimension. Feature extraction algorithms use domain transformation combined with statistical regularities to reduce data dimensionality and establish robust prediction or classification models. With the development of deep learning, neural networks such as CNN have also been widely used in DAS feature extraction.

Data denoising

The noise sources in the DAS system mainly include Gaussian noise caused by devices and the environment, phase noise introduced by the laser source, and two types of fading phenomena, namely, intensity fading and polarization fading [67]. Intensity fading is due to the interference between the backscattered signals of different scattering points within a single pulse. In Φ-OTDR systems based on heterodyne detection, the polarization mismatch between the local oscillator and the backscattered signal leads to the occurrence of polarization fading. When this fading occurs, the phase extracted at these fading points is destroyed by noise, making it difficult to locate vibration events and reducing the effectiveness of Φ-OTDR. Intensity fading can be mitigated by using multi-wavelength lasers, frequency scanning, or wavelength grading techniques simultaneously. The polarization fading effect can be reduced by polarization diversity technology.

Noise reduction algorithms are usually designed based on appropriate assumptions about the distribution of noise in time, space, and frequency domains. Common noise reduction algorithms include filtering, decomposition, image-based noise reduction algorithms, and deep learning methods. The advanced work in noise reduction in recent years is listed in Table 2. It is worth noting that the SNR in the table is not calculated in exactly the same way.

Filtering can filter out specific frequency ranges in the DAS signal, which is an effective way to suppress noise. Due to its simple operation and significant effect, it is often used in the noise reductio. For digital filtering of data, there are mainly FIR high-pass filters [7], which can suppress low-frequency noise, and band-pass filters [8, 9], which extract effective frequency components. In 2014, Li et al. [68] proposed a method based on power spectral analysis, which used the frequency characteristics of RBS light at the perturbation position to locate the vibration event and increased the SNR to 19.4 dB; in 2019, Zhang et al. [69] proposed a multi-dimensional matching filtering method, which can achieve a 5.76 dB SNR enhancement even for strong noise interference under suitable filter sizes.

Table 2 Recent Advancements in algorithm noise reduction

Ref	Method	Year	Initial SNR/dB	Improved SNR/dB	Data source
[14]	2D-ED	2013	6.56	8.4	Laboratory
[68]	Power spectrum analysis	2014	5.7	19.4	Laboratory
[10]	Curvelet	2017	3.0	7.8	Laboratory
[11]	EMD	2017	15.56	18.30	Laboratory
[15]	2D-ABLF	2017	6.43	20.83	Laboratory
[69]	MMF	2019	8.69	14.45	Laboratory
[12]	EMD-PCC	2021	7.32	13.68	Laboratory
[13]	EMD-TFPF	2021	7.6	37.6	Laboratory
[18]	NLMS	2022	8.4	22.31	Laboratory
[17]	NLM	2023	13.92	23.39	Laboratory
[19]	DL-TSD	2020	7.5	53.98	Laboratory
[20]	Supervised CNN for phase noise	2021	13.4	42.8	Laboratory
[70]	Semantic image segmentation	2022	7.76	37.84	Laboratory
[71]	DnCNN	2022	7.13	26.02	Laboratory
[72]	DAS-N2N	2023	1.89	26.29	Glacier microseismic
[73]	MSI-Net	2023	− 0.5132	19.0062	Synthetic DAS-VSP
[74]	CSANet	2024	5.94	30.80	Synthetic DAS-VSP
[75]	SDT	2024	-0.0394	12.0818	Synthetic seismic data
[76]	ABM3D	2024	1.77	40.6	Laboratory

Signal decomposition is to decompose the original signal into a series of sub-signals according to a specific method, and then obtain the denoised estimated signal through threshold or weighted superposition methods. The wavelet-transform [10] and empirical mode decomposition (EMD) algorithm has also been applied to DAS denoising due to its excellent signal processing performance and the characteristics of not requiring preset basic functions. In 2017, researchers used EMD to decompose the original RBS signal into a series of intrinsic mode functions (IMF) and residual components, achieving a 2.74 dB SNR improvement [11]. Denoising work based on empirical mode decomposition and Pearson correlation coefficient fusion (EMD-PCC) [12] and empirical mode decomposition and time–frequency peak filtering (EMD-TFPF) [13] algorithms were proposed in 2021. EMD-PCC can effectively recover the signal in different frequency interference and increase the SNR from 7.32 dB to 13.68 dB. The EMD-TFPF algorithm can increase the SNR to 37.6 dB under low-frequency vibration of 0.1 Hz.

Since DAS signals can form two-dimensional signals according to their spatial and temporal distributions, many image denoising methods can also be applied to this field. In 2013, Zhu et al. [14] proposed a Φ-OTDR SNR enhancement method based on two-dimensional edge detection (2D-ED), which uses the Sobel operator convolution to calculate the pixel value of the gray image and improves the SNR to 8.4 dB; in 2017, He et al. [15] proposed an image reconstruction algorithm based on adaptive two-dimensional bilateral filtering, which can smooth noise while retaining more details of the image. It can adaptively select parameters for different signals with faster and stronger robustness and improve the SNR by 14 dB in experiments; as a classic image denoising algorithm, non-local means (NLM) has also been proposed for parameter optimization in Φ-OTDR [16], which effectively improves the accuracy of measurement and positioning. In 2023, Li et al. [17] proposed a NLM image processing method to improve the SNR of the

Φ-OTDR system, and the SNR reached 23.39 dB. In 2022, Yu et al. [18] used an adaptive prediction denoising method based on normalized least mean square (NLMS) to reduce non-stationary noise, and the SNR increased from 8.14 dB to 22.31 dB.

In the past decade, machine learning and deep learning have played an increasingly important role in signal and image processing. Therefore, they have gradually been used in DAS data denoising. In 2020, Wang et al. [19] proposed an adaptive deep learning temporal-spatial detection (DL-TSD) method to extract vibration. They manually processed the waterfall chart, extracted the vibration, constructed a dataset, and trained CNN. In the best case, a super-high SNR of 53.98 dB can be obtained. In 2021, Jiang et al. [20] proposed a supervised learning-based method to suppress multiple phase noises. They constructed a dataset through numerical simulation and increased the SNR of the PZT vibration signal from 13.4 dB to 42.8 dB. In 2022, Li et al. [70] proposed a method based on semantic image segmentation. They annotated the vibration in the waterfall chart and trained it. The SNR can reach 37.84 dB. In the same year, the classic machine learning denoising algorithm Denoising CNN (DnCNN) was used in Φ-OTDR denoising [71]. The pure striped image is considered an ideal vibration image. By constructing a noise-clean image pair by superimposing real RBS noise on the striped image, the SNR was improved by about 20 dB.

DAS represents a novel technology for seismic data acquisition. Noise suppression is a crucial step in seismic data processing. The denoising process of DAS seismic signals encounters two primary challenges. Firstly, DAS seismic data contains certain background noises, such as optical low-frequency noise and fading noise, which are absent in conventional seismic data. Secondly, the SNR of DAS seismic data is relatively low. In recent years, neural networks have demonstrated superior denoising performance compared to traditional methods. Lapins et al. [72] introduced a weakly supervised machine learning method named "DAS-N2N" to suppress strong random noise in DAS signals. This method does not require paired clean and noisy signals for training. Instead, it utilizes two fibers within the same cable to record two noisy copies of the same underlying signal. Since random noise is independent, the deep learning model can be trained using only these two noisy data copies. The goal is to map the random noise process to selected summary statistics, such as the mean, median, or mode of the distribution, while preserving the true underlying signal. Once the model is trained, only noisy data from a single fiber is needed. Sui et al. [74] proposed a Cosine Spectrum Association Network (CSANet) for denoising DAS Vertical Seismic Profile (VSP) data. This algorithm considers both time shift and frequency information, achieving better recognition and recovery of weak DAS signals. Additionally, a feature fusion module was designed to ensure the entire network better utilizes composite information. CNNs have limitations in capturing long-range dependencies and maintaining global consistency, which restricts their effectiveness in DAS seismic data denoising. To address this, Wang et al. [75] proposed a transformer-based model called Seismic Data Denoising Transformer (SDT) for seismic signal processing. Utilizing the self-attention mechanism, the SDT model overcomes the limitations of CNNs, effectively capturing long-range features for seismic signal reconstruction. This approach also introduces a new self-supervised pre-training strategy using large-scale datasets to further enhance performance. Experimental results indicate that SDT excels in suppressing complex seismic noise and preserving weak signal

amplitudes. Wang et al. [73] proposed a Multi-Scale Interaction Convolutional Neural Network (MSI-Net) for the challenging task of DAS seismic data denoising. Unlike most existing CNN architectures for seismic data denoising, MSI-Net considers both coarse-scale and fine-scale features. It improves inherent serial convolutions to multi-scale parallel convolutions, which is beneficial for detail recovery. This approach uses specific connections to facilitate information interaction between different scales, promoting information flow and enabling the network to extract more information-rich multi-scale features from DAS seismic data.

Currently, traditional algorithms have poor denoising effects in low SNR environments. Compared with traditional image processing algorithms, machine learning usually performs better, but there are still problems such as complex training set construction and difficulty in model transfer in different scenarios in practical applications. To solve these problems, our research group proposed a Block-matching and 3D filtering (BM3D) method for distributed optical fiber sensing [45, 76, 77]. As shown in Fig. 6, the method is divided into two stages, each stage consists of grouping, collaborative filtering, and aggregation. First, find the matching block M similar to the reference block R in the image and integrate them into a three-dimensional array. Then, perform a three-dimensional transformation on the array, and use hard threshold filtering (or Wiener filtering) and inverse transformation operation in the second stage. After processing, return the block to the corresponding position in the original image. Finally, the estimated results of all overlapping blocks are weighted and averaged to obtain the estimated result of the real image (the estimated result of the first stage and the original noise image are used as the input of the second stage). This method can significantly reduce noise while retaining the details of the image by utilizing the correlation between data in the time and space domains. Without changing the original system structure, we achieved distributed vibration sensing with a spatial resolution of 20 m within a range of 50 km. The SNR at the end of the fiber increased from nearly 0 dB to 37.2 dB. Compared with traditional image denoising algorithms, the BM3D method has better denoising performance, and its processing process is more concise than that of deep learning-based methods. Based on these advantages, we believe that this method can be widely used to improve the SNR performance of Φ-OTDR, thereby achieving the goal of detecting small vibrations or extending the sensing distance.

Feature extraction

Using DAS data to identify and distinguish vibration events requires the extraction of relevant features from the data, which is often combined with domain transformation

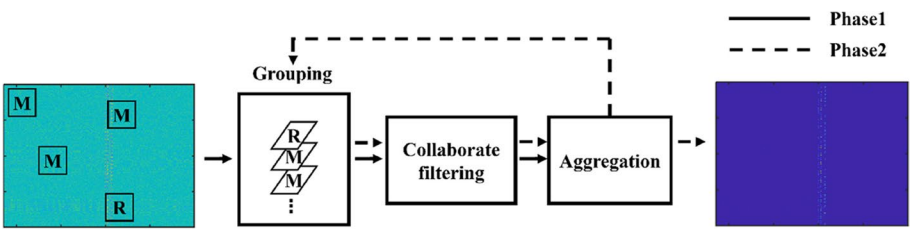

Fig. 6 Flowchart of the proposed BM3D denoising for Φ-OTDR [77]

techniques. The commonly extracted features can be roughly divided into statistical features, one-dimensional signal features, and image features. Statistical features are mainly used for traditional machine learning algorithms, such as SVM and XGBoost, etc. According to the different characteristics of time-domain and frequency-domain signals, corresponding features are selected. Time-domain features include peak-to-peak value, variance, mean, root-mean-square value, kurtosis, etc., which are similar in most work [21]. In addition to analyzing the spectral parameters, there are also some different extraction methods for frequency-domain features, such as dividing the spectrum into different frequency range intervals and calculating the energy of these intervals [21]. SVD decomposition of the spectrum is also used to select the largest few singular values [22]. In addition, statistical features such as wavelet entropy [21, 22], wavelet information quantum [21, 22], Hilbert transform and EMD [7, 46], Mel frequency cepstrum, Synchrosqueezing Transform [78], short-time Fourier transform [23, 24, 79], and Spearman correlation coefficient [80] can all be used for classification.

On the basis of single feature extraction methods, researchers have proposed many different ways to combine multiple features [81–83]. Du et al. [84] proposed a feature correction algorithm based on sample feature weighting method to effectively improve the performance of Φ-OTDR in complex environments. Huang et al. [85] proposes a pattern recognition method based on self-reference feature extraction. The proposed method constructs self-reference features from two dimensions of vibration and reference position, which improves the effectiveness of the features. At the same time, the abnormal data points are effectively filtered to further improve recognition accuracy.

Manual feature extraction can effectively improve the accuracy of classification, but it relies heavily on professional knowledge and has weak scene generalization ability. With the development of AI, deep learning models can extract features from one-dimensional signals or two-dimensional images by themselves and complete the tasks of classification and recognition. Machine learning techniques such as Principal Component Analysis (PCA) [86], 1D Residual Neural Network (1D-ResNet) [87], CNN [88–90], Long Short-Term Memory (LSTM) [91, 92] have been applied to feature extraction. The process of converting one-dimensional time series into two-dimensional images is essentially a dimensional increase, which means an increase in information content. At the same time, some features of the data can be better highlighted in the conversion process, and feature extraction and pattern recognition can be completed with the help of mature computer vision technology. Therefore, researchers are paying more attention to the construction of DAS two-dimensional images. Due to the spatiotemporal characteristics of DAS signals themselves, the common two-dimensional images are formed by stacking one-dimensional data after intensity demodulation according to the order of pulse emission [5, 8, 93, 94], and the envelope of the two-dimensional image can also be extracted on this basis to highlight the characteristics of the image [95]. Since the time–frequency characteristics of different vibration events will have significant differences, short-time Fourier transform [23, 24, 91], gammatone filter cepstrum coefficient envelope [96], Mel frequency cepstrum [1], and wavelet transform [91, 97] have also been used to construct two-dimensional images. Hu et al. [98] systematically evaluated the performance of various image encoding techniques, including GAF, Markov Transition Field (MTF), Recurrence Plot (RP), and Recurrence Plot Matrix (RPM), when integrated with deep learning

models. Their study provides a detailed comparison of these techniques in terms of their effectiveness and compatibility with deep learning frameworks.

MTF is a visualization technique used for dynamic system modeling and analysis. By converting time series data into two-dimensional images, it reveals the state transition rules and dynamic features in the system. Given a time series data, we can calculate the state transition probability between adjacent time points and represent these probability values as pixel values in the image [31, 99]. By using MTF, we can analyze time series data in an intuitive way and reveal important dynamic features in the sequence, as shown on Fig. 7. The image contains information about each sampling point and can be recognized by deep learning methods. Wei et al. [100] proposed a method that converts phase time series into MTF matrices, which are then combined with Non-negative Matrix Factorization (NMF) to generate RGB images. By leveraging 2D CNNs for classification, their approach demonstrated superior training efficiency and achieved over a 13% improvement in recognition accuracy compared to traditional 1D CNN methods.

GAF is a visualization technique used for time series analysis. GAF converts time series into two-dimensional images to capture potential patterns and relationships in the time series. Specifically, GAF uses the Gramian matrix of the time series to calculate the angle information at each time point, and then represents these angle information as pixel values in the image [25, 26], as shown in Fig. 8. This allows us to

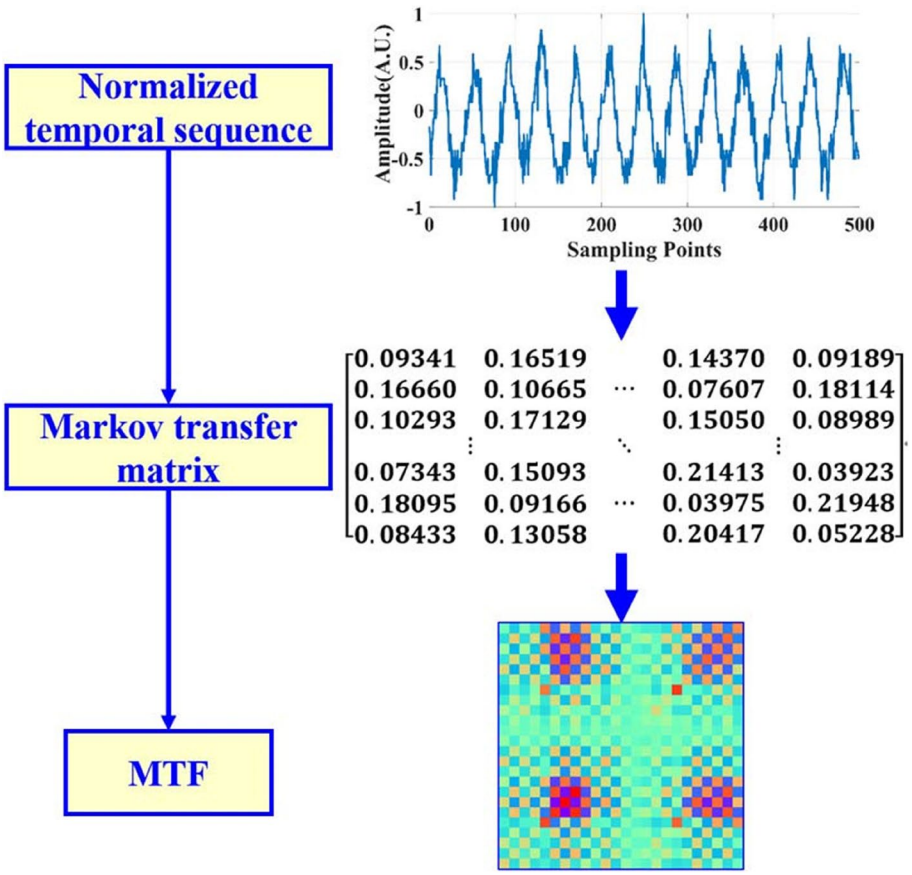

Fig. 7 The flow chart of transforming time series into MTF [31]

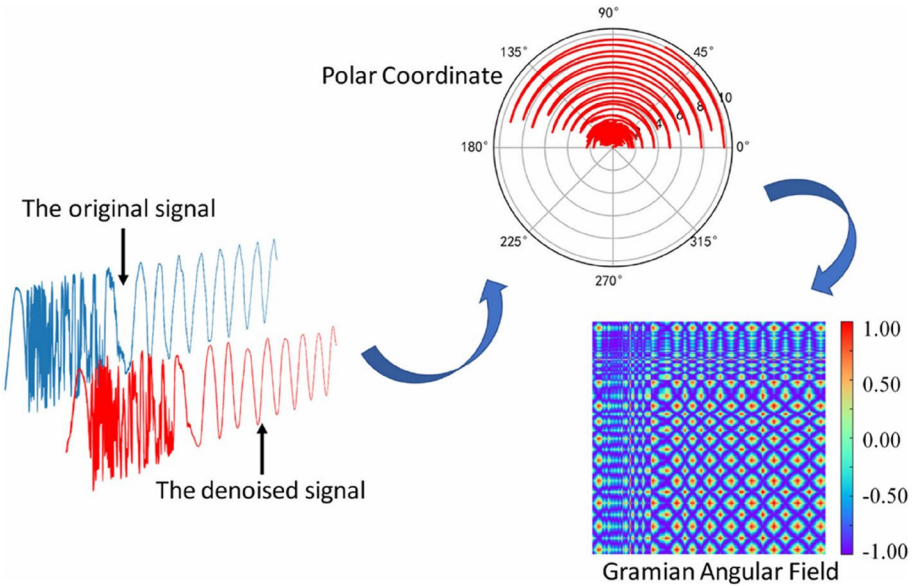

Fig. 8 DAS image construction based on GAF [25]

observe patterns and structures and to assist us in understanding the hidden dynamic features in the sequence. Wang et al. [101] utilized the Gramian Angular and Summation Field (GASF) algorithm to encode signals into two-dimensional image features. Combined with the ConvNeXt network and a cosine annealing optimization algorithm, their method achieved recognition accuracies of 99.3% for single-point disturbances and 98.3% for multi-point disturbances, with an average response time of 0.103 s. Hua et al. [102] developed the TFF-CNN framework, which integrates Gramian Angular Difference Field (GADF) encoding with FFT-based Co-occurrence Matrices (FFTT) to generate time–frequency feature images. This dual-channel model achieved a recognition accuracy of 99.30% with a response time of just 0.6 s, showcasing notable advantages in terms of low false alarm rates and minimal latency.

RP, also known as recurrence graphs, have important applications in time series analysis and nonlinear dynamics. RP visualizes repetitive patterns and similarities in time series by transforming them into two-dimensional matrices. Specifically, given a time series, we can calculate the similarity measure between different moments in time according to a certain algorithm, and then visualize the similarity matrix as a graph, which is the RP. The generation of RP first selects an appropriate similarity measure method and calculates the similarity between different moments in time on the time series. Then, the similarity matrix is transformed into a graph, usually in the form of a black-and-white block matrix, where black blocks represent pairs of moments with high similarity, and white blocks represent pairs of moments with low similarity, as shown in Fig. 9 [103]. RP can be used to discover important information such as periodic patterns, similarity patterns, and chaotic dynamics in time series. By observing the structure and features of RP, important dynamic characteristics of time series can be revealed, which can help better understand and analyze complex time series data and extract useful information.

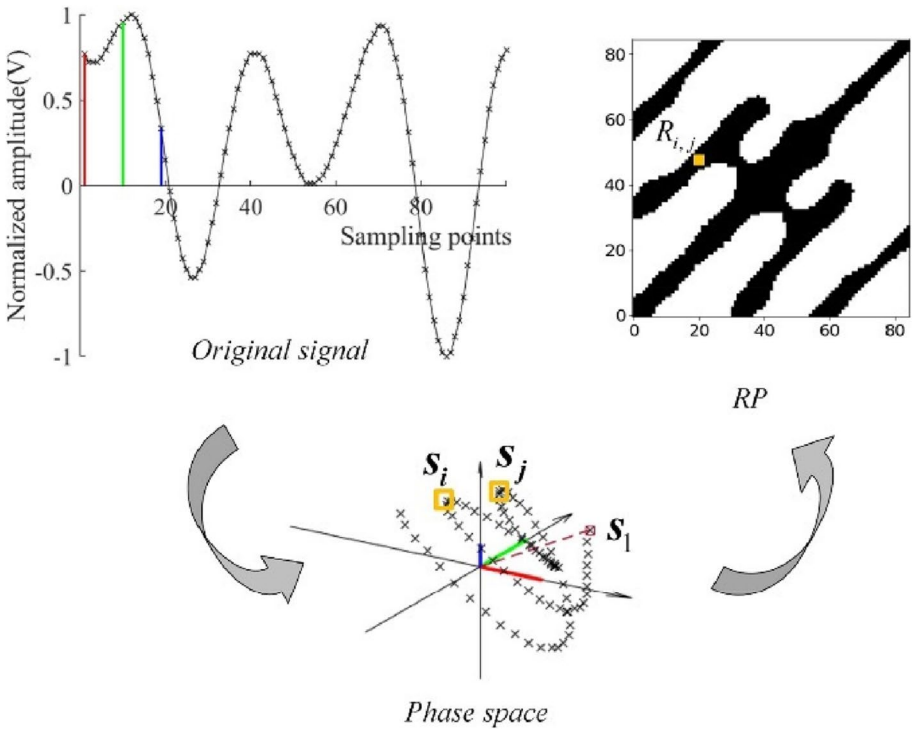

Fig. 9 DAS image construction based on RP [103]

Classification / recognition models

Traditional machine learning

Traditional machine learning refers to the use of mathematical methods such as statistics, linear algebra, and optimization algorithms to learn from existing data and construct predictive models for predicting and classifying unknown data. SVM [7, 21, 27], HMM [28–30], the ELM classifier with the fisher score feature selection method (F-ELM) [22], Dendrite Net [104], and XGBoost [105] are all used for DAS signal recognition and classification. A summary of machine learning pattern recognition is shown in Table 3.

SVM are a commonly used machine learning method that is widely used in pattern recognition, data classification, and regression. Its basic idea is to achieve classification by finding an optimal hyperplane that can separate samples of different categories and has the maximum margin, so that the generalization performance of the classifier is optimal. In SVM, samples are viewed as points in feature space and labeled according to their categories. By mapping samples to a high-dimensional feature space, SVM is essentially looking for an optimal hyperplane that maximizes the margin separation of samples on the hyperplane. These sample points with the maximum margin on the hyperplane are called support vectors, and they play a key role in determining the decision boundary. The core of SVM is to map input samples to a high-dimensional feature space through a kernel function, which can handle nonlinear problems.

Commonly used kernel functions include linear kernel, polynomial kernel, and radial basis function (RBF) kernel, etc. These kernel functions can map samples from low-dimensional space to high-dimensional space and perform classification in

Table 3 Summary of machine learning DAS pattern recognition

Ref	Year	Preprocessing	Input	Network	Training dataset	Application scenario (Number of events)
[27]	2019	WPD denoising	T	1D CNN + SVM	Field: 7762	Buried pipeline safety monitoring(5)
[28]	2019	---	F	GMM-HMM	Field: 35680	Buried pipeline safety monitoring(4)
[29]	2019	Feature extraction	Features from T, F and T-F	HMMs	Field: 267	Buried pipeline safety monitoring(5)
[22]	2020	Feature extraction	Features from T and F	F-ELM	Field: 525	Airport perimeter intrusion monitoring(5)
[7]	2020	High-pass filter	T-F	TFDC-SVM	Field: 255	Submarine cable shock events of different magnitude(3)
[105]	2020	EMD-CIIT denoising Feature extraction	Features from T, F and T-F	XGBoost	Field: 900	Railway intrusion monitoring(5)
[21]	2021	Feature extraction	Features from T and F	NC-SVM	Field: 450	Vibration events(5)
[30]	2021	Feature extraction	Features from T	mCNN-HMM	Field: 11916	Underground communication cables monitoring(4)
[104]	2023	Feature extraction	Features from T	VTTCG-DD	Lab: 12478	Vibration events(6)

T represents the time domain signal, F represents the frequency spectrum, T-F represents the time–frequency spectrum

Field represents data from real-world scenarios, while Lab represents data from laboratory settings

"---" indicates not available

high-dimensional space. By selecting the kernel function and adjusting the hyperparameters reasonably, SVM can fit various complex nonlinear patterns. SVM has a solid theoretical foundation and strong generalization ability and can handle classification tasks in high-dimensional data and small samples. In addition, by introducing soft margin and kernel tricks, SVM can also handle some linearly inseparable problems. Jia et al. [21] proposed near category support vector machines (NC-SVM) by combining K-nearest neighbor (KNN) to extend binary SVM to multi-class problems. Compared with other multi-class SVMs, it effectively improves the classification accuracy. Fouda et al. [7] combined time–frequency domain features with SVM classifiers to identify malicious attacks on multiple submarine cables, as shown in Fig. 10. The classification accuracy of three typical events reached more than 96%. However, there is still room for improvement in the classification accuracy of another event. Wu et al. [27] proposed a method of feature extraction based on 1D-CNN combined with SVM classification. Use efficient 1-D CNN to replace 2-D CNN for feature extraction; then use SVM classifier to replace the softmax layer in the CNN network to further optimize the classification. The recognition accuracy in the oil pipeline monitoring application reaches more than 98%, which is better than the typical fixed-feature machine learning method and the deep learning method related to 2-D CNN.

HMM is a commonly used probabilistic graphical model, which is widely used in speech recognition, natural language processing, image processing, and other fields. HMM models are based on the hidden states of Markov processes and predict hidden states based on observed output sequences. An HMM contains two basic parts: hidden

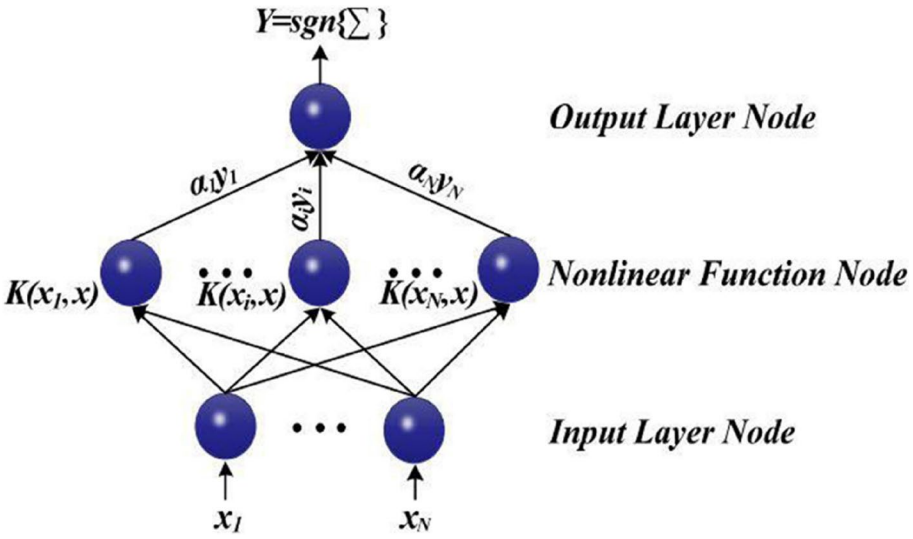

Fig. 10 The architecture of SVM [7]

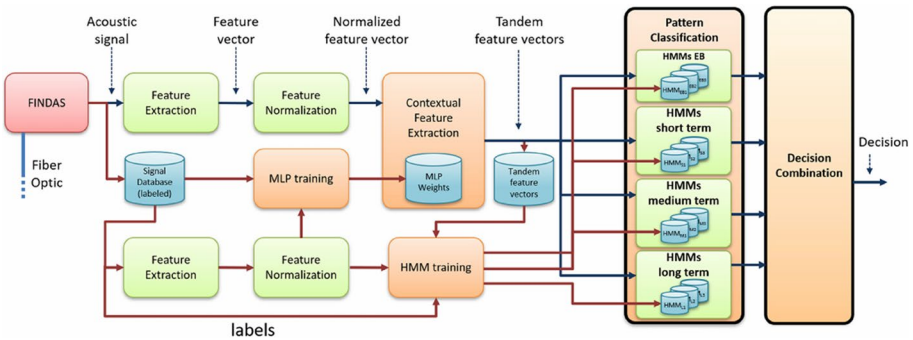

Fig. 11 GMM-HMM pattern recognition model (HMMs EB: Hidden Markov Models Empirical Bayes) [28]

states and observation sequences. Hidden states are invisible states in the time series, while observation sequences are visible outputs associated with hidden states. HMM assumes that the current state is only related to the previous state, that is, it satisfies the Markov property. This means that for the state at any time, its transition probability is only related to the previous state and is independent of other states or observations. The application of HMM models mainly include evaluation problems (calculating the probability of the observation sequence) and decoding problems (solving the most likely hidden state sequence). Based on these problems, we can perform signal recognition, sequence labeling, and other tasks. Tejedor et al. [28] introduced feature-level contextual information in the Gaussian Mixture Model-Hidden Markov Model (GMM-HMM) based pattern classification system and used a system combination strategy for decision-making, as shown in Fig. 11. System combination depends on the majority of decisions given by a single contextual information source and the number of states used for HMM modeling. The system runs in two different modes: the first is the machine + activity recognition mode, which recognizes the activity being performed by a machine; the second is the threat detection mode, which detects threats regardless of the actual activity being performed. Compared with the systems previously based on the same strict

experimental settings, the system combination based on contextual feature information and GMM-HMM method improved the results of machine + activity recognition and threat detection. Tejedor et al. [106] proposed a hybrid model for threat recognition, which integrates a random forest-based feature extraction method, a multi-layer perceptron (MLP) classifier, and a parallel GMM-HMM for pattern classification. To enhance decision-making, the system employs a majority voting strategy that combines outputs from various feature extraction methods and GMM-HMM classifiers configured with different state numbers. Experimental results demonstrate that the proposed system outperforms previous methods, achieving a 5% relative improvement in machine and activity recognition, a 1% increase in pipeline threat detection rate, and a 15% reduction in false alarm rate.

Supervised deep learning

Deep learning is a machine learning method based on artificial neural networks. It can perform feature learning and pattern recognition in an unsupervised or supervised manner by connecting multiple layers of neurons and adjusting their weights. Traditional acoustic pattern recognition methods usually rely on manually extracted features, which are limited by the need for a lot of domain knowledge and professional experience and are not suitable for complex and diverse datasets. The advantage of deep learning is that it can automatically learn features from raw data and perform efficient pattern recognition. Neural networks such as artificial neural networks (ANN) [57], Spiking Neural Networks (SNN) [23], multi-layer perceptron neural networks (MLPNN) [107], PNN [86], and CNN [25, 26, 31] have been used for DAS signal pattern recognition. A summary of deep learning pattern recognition is shown in Table 4.

CNNs are a widely adopted deep learning model in computer vision and pattern recognition, characterized by their ability to extract features through convolution operations and represent complex patterns using multi-layer neural networks. The fundamental principle of CNNs lies in constructing hierarchical features through multiple convolutional and pooling layers. In convolutional layers, a set of learnable convolutional kernels performs convolutions on the input data, capturing local features from images or other input patterns. By leveraging weight sharing and local connections, convolutional kernels significantly reduce the number of parameters, improve computational efficiency, and enhance the model's generalization capabilities. Pooling layers, on the other hand, perform down-sampling and feature compression by applying operations such as max pooling or average pooling. These layers reduce the spatial dimensions of feature maps while preserving essential features, thereby lowering computational costs and improving the model's robustness to spatial translations. In addition to convolutional and pooling layers, CNNs also include fully connected layers and activation function layers. Fully connected layers link the extracted features to output categories, enabling tasks such as classification or regression. Activation function layers introduce nonlinearity into the model, allowing it to learn more complex patterns. A typical CNN architecture for DAS event classification [26] is illustrated in Fig. 12. In this approach, phase signals are converted into two-dimensional images using GAF, labeled to construct a dataset, and subsequently fed into the convolutional neural network for pattern recognition. Wu et al. [1] proposed an intensity and phase superimposed CNN (IP-CNN) to use the intensity and

Table 4 Summary of deep learning DAS pattern recognition

Task	Ref	Year	Preprocessing	Input	Network	Training dataset	Application scenario (Number of events)
Classification	[25]	2020	Wavelet denoising Image coding	GAF	CNN	Field: 4800	Intrusion events (6)
	[108]	2020	---	S-T	CNN-LSTM	Field: 123	Intrusion event under strong noise interference of high-speed railway (3)
	[109]	2020	---	T	CPL-MSCNN	Field: 4800 (known) 0 (unknown)	Intrusion events (6 known, 4 unknown)
	[93]	2021	Image coding	GSIs	2DCNN-LSTM	Field: 2624	Perimeter security events (7)
	[110]	2021	Band-pass filter	S-T	CNN	Field: –-	Seismic; Noise
	[107]	2021	---	Power spectrum	MLPNN	Field: 12,640	Road intrusion events (6)
	[86]	2021	Feature extraction	Features from T	PCA-PNN	Lab: 525	Disturbance event (5)
	[31]	2022	Image coding	MTF	CNN	Lab: 1373	Disturbance event (5)
	[26]	2022	Image coding	GAF	CNN	Field: 4390	Intrusion events (6)
	[111]	2022	---	T	ATCN-SA-BiLSTM	Field: 1120	Perimeter security events (4)
	[112]	2023	Band-pass Filter Feature extraction	Features from T	1D-RL-CNN with OpenMax	Field: 1188 (known) 0 (unknown)	Road intrusion events (3 known, 3 unknown)
	[88]	2023	Denoising	T-F	CNN Bi-LSTM-CLC	Lab: 6850	Vibration events of different frequencies (5)
	[113]	2023	High-pass filter	T	CDIL-CBAM-BiLSTM	Lab: 5040	Perimeter security events (6)
	[114]	2024	Sliding average method	T	APL-1D ResNet	Field: 4230	Pavement damage events (6)
	[102]	2024	Denoising Image coding	GADF FFT^T	TFF-CNN	Field: 600	Intrusion detection (5)
	[101]	2024	Wavelet denoising Image coding	GASF	GASF-ConvNeXt-TF	Lab: 6480	Intrusion events (6)
	[98]	2024	Wavelet denoising Image coding	GAF, MTF RP, RPM	NAM-HorNet	Lab: 11,540	Intrusion events (6)
Object detection	[115]	2022	Moving average method	S-T	YOLO	Lab: 4050	Perimeter security events (5)
	[116]	2022	Median Filtering Pseudo-Color Processing	S-T	YOLO-A30	Lab:8069	Perimeter security events (5)
	[97]	2023	synchrosqueezed wavelet transform	T-F	YOLOXs	Lab: ---	Steel Wire break detection in prestressed concrete cylinder pipes

Table 4 (continued)

Task	Ref	Year	Preprocessing	Input	Network	Training dataset	Application scenario (Number of events)
	[117]	2023	Band-pass filter Image Augmentation	S-T	Double-YOLO	Field: 2051	Footsteps detection
	[118]	2023	Band-pass filter	S-T	YOLOv5	Field: 10,000	Traffic detection (2)
	[119]	2024	Moving average method	S-T	CBAM-YOLOv8	Field: 32,432	TPerimeter security events (6)
	[120]	2024	---	S-T	ResNet50 Faster R-CNN	Field: 71 (set 1) 455 (set 2)	Intrusion detection (4)

T represents the time domain signal, F represents the frequency spectrum, T-F represents the time–frequency spectrum, and S-T represents the Spatio-temporal image

Field represents data from real-world scenarios, while Lab represents data from laboratory settings

"---" indicates not available

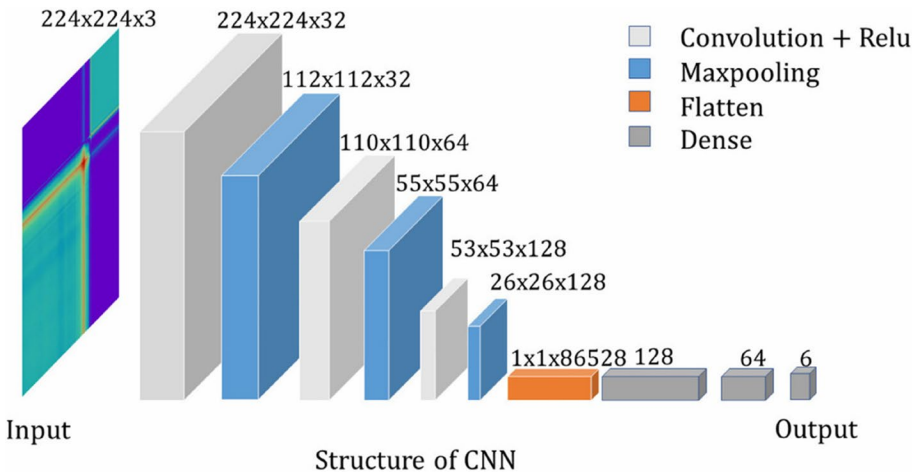

Fig. 12 Structure diagram of CNN [26]

phase information of DAS with coherent detection. The enhanced training dataset can greatly improve the classification accuracy.

Deep learning methods improve the accuracy of event recognition and can automatically extract features based on sample distribution. However, almost all these methods focus on closed-set recognition and cannot recognize signals of unknown categories that are not involved in model training. In practical applications, due to the complexity of the environment around the sensing fiber, the types of signals are more than those that can be used in training. Therefore, when the closed-set recognition model is applied to an open-set environment, unknown events will be misclassified as known categories, thereby reducing the recognition accuracy of the sensing system. To overcome this defect, Zhou et al. [112] proposed an open-set event classification model for distributed fiber-optic vibration sensing system based on 1D residual

learning convolutional neural network (1D RL-CNN) and OpenMax algorithm, which can handle signals of known and unknown categories. Cars, excavators, road breakers and other events with high threats are used as known samples for model training and closed-set recognition, while walking, running, environment and other events with low threats are used as unknown samples for open-set recognition. The experimental results show that compared with the traditional one-dimensional CNN signal classification method, the classification accuracy of the recognition model has been greatly improved. Jiao et al. [114] proposed a convolutional neural network-based deep learning model, termed Anchor Point Learning (APL), designed to enhance the robustness of open-set recognition and minimize the overlap between known and unknown categories. APL assigns categories to distinct regions in the output space using anchor points and incorporates an adversarial regularization term to improve the compactness of intraclass features. In experiments on pavement intrusion signal recognition, APL demonstrated superior performance compared to the traditional Softmax method and state-of-the-art open-set recognition approaches, achieving effective intrusion recognition with a low false alarm rate in open-set environments.

Multi-Scale Convolutional Neural Network (MSCNN) can capture microscopic and macroscopic features in images by performing multi-scale convolution and feature extraction, thereby improving the recognition and segmentation capabilities of the model in complex scenes. Lyu et al. [109] proposed a robust intrusion event recognition scheme based on the convolutional prototype network (CPL), which integrates the relevant variables learned by the prototype into the training process of the MSCNN as trainable parameters. This scheme realizes end-to-end feature extraction and recognition based on the similarity of intrusion signals and has the ability to recognize and reject unknown interference events. In field experiments, the average recognition accuracy of known intrusion events can reach 84.67%, and the rejection rate of unknown interference events is about 83.75%, ensuring the accuracy of intrusion event monitoring in complex field environments. Wu et al. [30] designed an improved multi-scale convolutional neural network (mCNN) to automatically extract the local structural features of DAS signals from multiple perspectives. Then, the HMM is used to mine the sequence information of the previously extracted features of the entire sample. Based on the test results of actual field data, this method is superior to HMM models with comprehensive manual features, CNN-HMM models, and MS-CNN-HMM models in terms of feature extraction. In addition, the Euclidean distance between the posterior probabilities of correct classification and error classification was proposed to evaluate the feature distinguishability of test samples under different recognition models. Then, an objective parameter was used to measure the feature extraction ability of the model.

LSTM is a widely used recursive neural network model in the field of sequence data analysis and natural language processing. LSTM can adaptively control the flow and retention of information by introducing three gating units (input gate, forget gate, and output gate). The gating mechanism can learn the weights and biases of the gating units based on the content and context of the input data, thereby realizing the modeling of long-term and short-term memory, as shown in Fig. 13. To address the issue of low recognition accuracy in high-sampling-rate long-sequence signal data collected by the DAS system, Wang et al. [113] proposed a circular dilated-convolutional block

attention module- Bi-LSTM (CDIL-CBAM-BiLSTM) network model that leverages feature fusion. This model employs an improved circular dilated convolutional neural network to extract detailed temporal structure information from each signal node. It then integrates this information with a bidirectional LSTM network to perform deep data mining through feature fusion. Additionally, to enhance the model's performance, a convolutional block attention module is incorporated. Experimental results, based on 5040 training samples and 2160 test samples, demonstrate that the model achieves an average recognition accuracy of over 99% for six real interference events in perimeter security scenarios, with a recognition time of less than 2 ms. The combination of CNN and LSTM is widely used in DAS pattern recognition [88, 111, 113, 121], including pipeline safety monitoring [91], earthquake [110] intrusion events [93, 108, 122], etc.

Deep learning algorithms have been extensively applied to DAS event classification tasks. However, practical DAS applications often demand not only accurate event classification but also precise event localization. For instance, in scenarios such as pipeline leakage monitoring or perimeter security, localization information is critical for enabling rapid responses. Consequently, object detection algorithms, which integrate event recognition and localization, have emerged as a key research focus in the DAS field.

Faster R-CNN, a classic algorithm in object detection, utilizes a Region Proposal Network (RPN) to generate candidate regions and combines CNNs to jointly optimize object classification and localization. This approach significantly enhances detection accuracy and efficiency. In DAS systems, Faster R-CNN has been widely adopted for anomaly detection in complex environments due to its precise localization capabilities. For example, Li et al. [120] proposed a Faster R-CNN-based monitoring framework that employs two collaborative Faster R-CNN models, along with max-pooling layers and monitoring strategies, to effectively identify and locate construction activities. Within a 5.25-km fiber range, the framework achieved a recognition rate of 98.85% for construction activities while reducing processing time to 6.6 min, demonstrating improved real-time performance. Compared to traditional classification algorithms, Faster R-CNN exhibits superior capabilities in event detection and localization, particularly when handling large-scale spatiotemporal data.

YOLO (You Only Look Once) is a highly efficient real-time object detection algorithm that excels in both speed and accuracy. By framing object detection as an end-to-end regression task, YOLO employs a grid-based prediction mechanism and

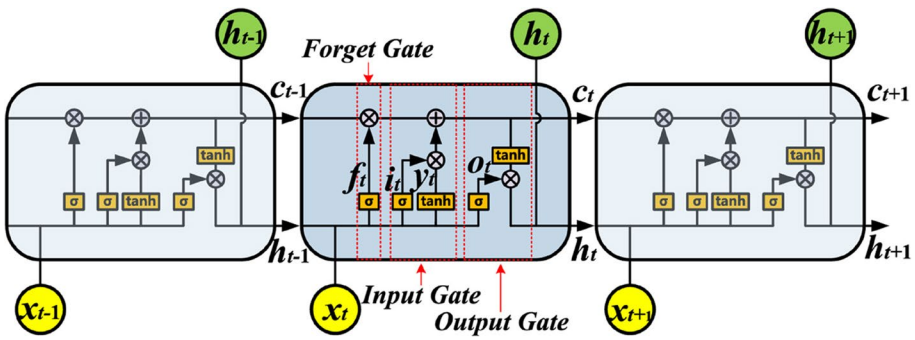

Fig. 13 Long short term memory network architecture [93]

multi-scale feature extraction to achieve real-time and accurate detection. Variants such as YOLO-v3 [123], YOLO-v5 [118], YOLO-v8 [119, 124], YOLO-A30 [116], YOLO-X [97], and double-YOLO [117] have been successfully applied to DAS object detection tasks.

In this study, we propose a real-time multi-class interference detection algorithm based on YOLO, which is shown in Fig. 14[115]. Using the Φ-OTDR system, 5,787 samples covering five types of perimeter security events were collected and preprocessed into images, which were manually labeled to create a dataset. The proposed method adopts the Darknet53 network structure, simplifying the traditional two-step object detection process into a single-step approach that enables simultaneous event localization and classification. Additionally, the algorithm incorporates a Feature Pyramid Network (FPN) to enhance detection performance through multi-scale feature representation. Experimental results demonstrate that the proposed method achieves an accuracy of 96.14% at a detection speed of 22.83 frames per second, making it 44.90 times faster than Fast-RCNN and 3.79 times faster than Faster-RCNN. Furthermore, the method excels in detecting small objects, making it well-suited for real-time monitoring in complex environments. This approach provides an efficient solution for industrial Φ-OTDR online monitoring systems.

Advanced learning paradigms for DAS

Supervised learning methods depend on large volumes of labeled data to achieve high recognition accuracy. However, the lack of high-quality datasets in the DAS field complicates model training and validation. The substantial data volume resulting from DAS's high spatiotemporal sampling rate leads to high labeling costs and time-consuming processes, while the complex and variable application scenarios hinder the model's generalization ability. Consequently, supervised learning often faces low recognition accuracy in practical applications. To address these issues, advanced learning paradigms such as

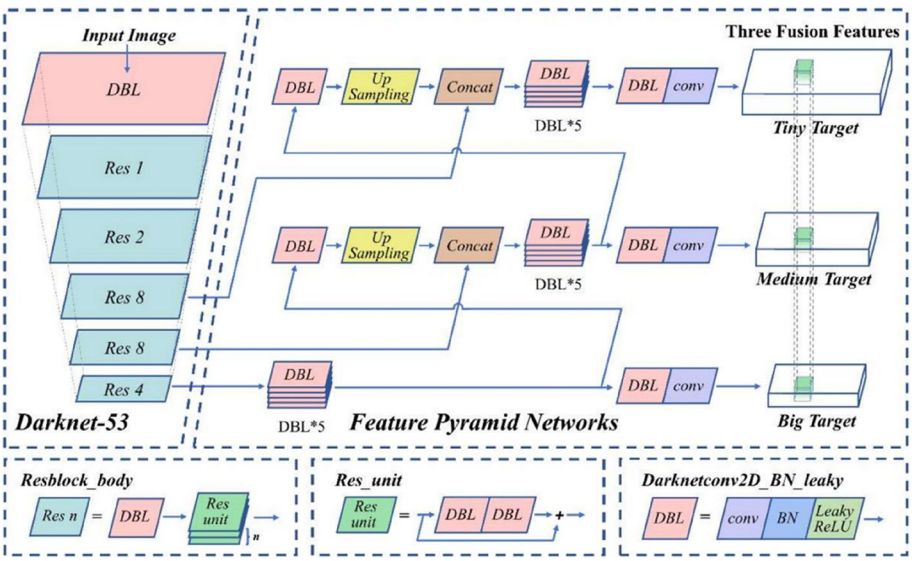

Fig. 14 YOLO architecture (DBL: Darknetconv2d_BN_Leaky) [115]

semi-supervised, unsupervised, incremental learning (IL), zero-shot learning (ZSL), few-shot learning (FSL) and transfer learning have been increasingly applied to DAS event recognition, aiming to achieve high-accuracy recognition of DAS events and robust generalization in complex scenarios using large amounts of unlabeled data and minimal or no labeled data.

Semi-supervised learning aims to enhance the model's generalization ability by leveraging large amounts of unlabeled data alongside a small amount of labeled data. This approach combines the strengths of supervised and unsupervised learning, significantly improving model performance when labeled data is scarce. The basic principles of semi-supervised learning are shown in Fig. 15. He et al. [125] proposed a semi-supervised model based on GAN. This method uses the GAN generator to provide a large volume of unlabeled data for the discriminator model, thereby overcoming the limitations of DAS supervised models with few labeled samples. Yang et al. [126] trained a Sparse Stacked Autoencoder (SSAE) using unlabeled data to extract robust DAS signal features and employed a small amount of labeled data to train a fully connected network for target localization and recognition. This method significantly enhances the utilization of unlabeled data and the model's adaptability across different scenarios. However, when the sample distribution is imbalanced, these semi-supervised learning methods may cause the model to favor categories with more labeled samples, resulting in poor performance for categories with fewer labeled samples. Wang et al. [127] proposed a semi-supervised learning method based on FixMatch. This method employs a consistency regularization mechanism to address label noise and uses data augmentation to expand the minority class sample dataset, thereby balancing the dataset's sample category distribution and enhancing the model's robustness. Li et al. [128] proposed a semi-supervised learning-based model that achieves significant improvements in event classification performance. The model integrates temporal feature extraction, bidirectional spatial feature representation, and a dual-attention mechanism. Under the condition of using only 1230 labeled samples, the model achieved a classification accuracy of 96.9%. Furthermore, it retained strong performance even as the number of labeled samples decreased, demonstrating its robustness in low-resource scenarios. Shi et al. [129] introduced a data selection

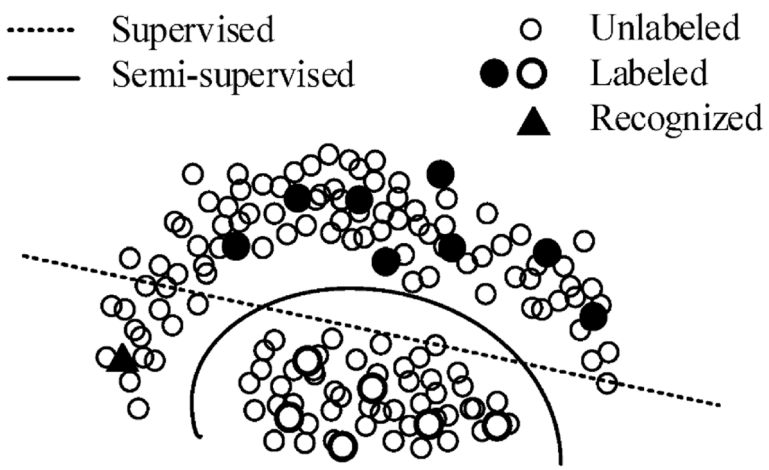

Fig. 15 The decision boundary reinforcement by semi-supervised learning [127]

approach driven by uncertainty estimation. This method identifies and selects the most informative samples from an unlabeled dataset, labels only these selected samples, and incorporates them into the training process. By doing so, it effectively reduces labeling costs while preserving classification accuracy, providing a cost-efficient solution for training high-performing models.

Unsupervised learning does not rely on pre-labeled data for model training but instead learns from the intrinsic characteristics of the data, automatically uncovering the underlying structure to classify specific events. Additionally, unsupervised learning can utilize all available data, unrestricted by the quantity and quality of labeled data, making it particularly advantageous for handling large-scale DAS data. Almudévar et al. [130] used an unsupervised autoencoder to detect DAS abnormal events, treating potential vibration events as anomalies and using only non-event signals for unsupervised deep learning. The main advantage of this method is that it does not require manual labeling, expanding its applicability for event detection in real environments without prior knowledge of potential events. However, this method currently can only identify the presence of abnormal vibration events and cannot further classify these events. Peng et al. [131] used unsupervised Self-Organizing Maps (SOM) and autoencoders to identify seven types of events. SOM is an effective unsupervised learning technique that uses neuromorphic principles to make adjacent neurons sensitive to similar inputs, with fast training speed. During training, SOM selects the neuron whose weight is closest to the input data, known as the Best Matching Unit (BMU), and updates the weights of each neuron to approximate the input data, with neurons closer to the BMU undergoing more significant weight updates. Experiments show that this method can achieve a recognition accuracy of 71%, likely due to underfitting in the absence of actual label feedback, making it difficult for the algorithm to distinguish between highly similar events. Zhang et al. [132] used PCA to reduce the dimensionality of DAS vibration event time-domain waveforms and then used the k-means algorithm to cluster five types of vibration events. Compared with the actual categories of vibration events, an equivalent classification accuracy of 99.4% was obtained. The Calinski-Harabaz index (CH) and Silhouette coefficient were also used to evaluate clustering performance. This clustering method has been shown to effectively perform unsupervised self-classification of DAS events. By simply observing or calibrating different clustering results, self-recognition in practical application scenarios can be achieved. Wu et al. [23] proposed an unsupervised learning method of SNN that approximates the brain's working mechanism to improve the model's generalization ability in different scenarios. The network structure is simple, including an input layer, an activation layer, and an inhibition layer. Each layer in the activation and inhibition layers consists of two basic units: neurons and synapses. The synapses connecting the neurons express the conductivity strength of the pulse transmission from the front neuron to the rear neuron. The input signal is converted into a pulse sequence through the control of the activation and inhibition layers, and finally classified according to the distribution of the pulse sequence. On inconsistent bad sample datasets and unbalanced datasets, unsupervised SNN is more stable than supervised CNN, with significantly improved generalization ability. Duthé et al. [133] proposed a new unsupervised machine learning method. This method uses a Transformer neural network adapted to time series to extract high-frequency information in DAS signals

and employs a contrastive learning scheme for training to learn coherent data representations. This latent representation can be used for unsupervised anomaly detection, reducing the need for expensive labeled offshore anomaly data.

ZSL and FSL are designed to mitigate the reliance of deep learning on large-scale labeled datasets. ZSL leverages prior knowledge to recognize unseen classes, making it particularly suitable for scenarios characterized by frequent emergence of novel events or high labeling costs. However, its performance is highly dependent on the quality of the semantic space. In contrast, FSL enables rapid adaptation to new classes with only a few labeled samples, offering significant flexibility. Nevertheless, it is prone to overfitting in scenarios involving a large number of classes or complex signal patterns. In the context of DAS, both methods effectively address the challenges posed by the diversity of event signals and the difficulty of obtaining labeled data. However, there remains a need to develop efficient models capable of handling high-dimensional signals and mitigating noise interference. To address the challenge of limited training samples in Φ-OTDR event recognition, Shi et al. [134] proposed a feature synthesis approach that integrates hybrid class strategies with reinforcement learning. In an eight-class event classification task involving unknown classes, their method achieved an average classification accuracy of 42% for unknown classes and an overall accuracy of 74%, representing improvements of 29% and 7%, respectively, compared to conventional methods. Notably, this approach was the first to enable recognition of specific events without requiring pre-collected samples. Hu et al. [135] introduced an Attribute Point Loss-based ZSL 1D Residual Network (APL-ZSL-1DResNet). Experimental results on both custom and public datasets demonstrated that this method achieved average recall rates of 75% and 66% for zero-shot events, and 94.6% and 83.5% for common events, respectively. These results highlight the superior performance of the proposed method in scenarios with limited labeled samples. Furthermore, Luong et al. [136] developed a few-shot classification framework tailored for urban infrastructure monitoring. This framework employs an embedding network to extract features and utilizes a classifier to perform few-shot classification tasks. The study also investigated three different data preprocessing techniques as input methods. Experimental results demonstrated that the framework achieved outstanding few-shot classification performance across multiple event categories, underscoring its potential for applications in urban monitoring.

IL has attracted increasing attention in DAS applications. Its primary goal is to enhance the training efficiency and adaptability of traditional deep learning models when encountering new events or shifts in data distribution, while simultaneously preventing the forgetting of previously acquired knowledge. In DAS systems, event categories are often dynamic and imbalanced. The frequent occurrence of new events and environmental changes poses significant challenges to the generalization capabilities of models. IL offers an effective approach to address these issues. Wu et al. [137] proposed an intelligent distributed acoustic sensing system (sDAS) based on multi-task learning (MTL) to tackle the challenges of event category imbalance and new event recognition. Their approach categorizes events into core events (requiring both recognition and localization) and non-core or new events (requiring only recognition). By freezing the shared and localization networks while fine-tuning only the recognition network, the method significantly enhances the recognition performance for new events. At the same

time, it maintains high-accuracy recognition (99.46%) and localization (error ± 1 m) for core events. Furthermore, the method is computationally efficient, making it suitable for real-time processing. For energy pipeline threat detection, Zhu et al. [138] developed a model based on Multi-dimensional Information Fusion and Broad Learning System (MIFBLS). This model integrates signal preprocessing, feature dimensionality reduction, and time–frequency map fusion, and employs a BLS IL strategy to alleviate the computational burden associated with data increments. Experimental results on real pipeline datasets demonstrated that the proposed method significantly improves recognition efficiency and accuracy, reduces false alarm rates, and satisfies the requirements for real-time monitoring. Liu et al. [139] introduced an IL framework for ϕ-OTDR systems, which combines an optimized "Learning without Memorization" (LwM) algorithm with an improved ConvNeXt network. The framework incorporates a High-Efficiency Channel Attention (HECA) mechanism to extract spatiotemporal features and leverages knowledge distillation and Gradient-weighted Class Activation Mapping (Grad-CAM) to mitigate the forgetting of previously learned information. Experimental results showed that the framework achieved a recognition rate exceeding 93% for 10 types of intrusion signals, reduced the forgetting rate from 41.44% to 5.25%, and enabled real-time IL on edge devices. These results highlight its potential for deployment in resource-constrained environments.

Supervised and unsupervised learning often require training models from scratch when applied to new fields or different scenarios, leading to time and resource inefficiencies in data collection and labeling. Transfer learning can significantly reduce the need for labeled data in the target domain and accelerate the model training process by transferring pre-trained models or features from the source domain to the target domain, achieving faster convergence and higher accuracy in the target task. Gan et al. [140] utilized transfer learning within the VGGish framework to extract high-dimensional frequency-domain features from signals. To enhance the representation of these features, the spatial distribution characteristics of multiple acquisition points were integrated, enabling the fusion of spatiotemporal features. These fused features were further refined using a sample feature correction algorithm. Finally, a SVM classifier was applied to perform event recognition. With only 960 training samples, this method achieved a recognition accuracy of 95.0% across six types of intrusion events, demonstrating its effectiveness as a solution for optical fiber sensing event recognition under small-sample conditions. Shi et al. [8] proposed a DAS transfer learning method based on pre-trained AlexNet. The AlexNet network is pre-trained using a large-scale image dataset, and then the model is retrained and fine-tuned using DAS signal samples to achieve rapid learning and classification on small-scale datasets in new scenarios. To further reduce the training time for model deployment, Li et al. [141] used SVM for event classification based on the feature extraction of DAS signals using the pre-trained AlexNet model. Without using a graphics processing unit (GPU), the new recognition model is obtained by retraining only the SVM classifier, reducing the training time of the new model to meet the real-time monitoring needs of small embedded devices, thereby further lowering the threshold for the use of deep learning. Additionally, some lightweight deep learning models [24, 99, 142] can significantly reduce the demand for computing and storage resources, improve inference speed, reduce energy consumption, and be suitable for

various hardware platforms with their advantages in resource saving, real-time performance, energy consumption reduction, and deployment flexibility, and are widely used in DAS practical engineering scenarios.

A summary of advanced learning paradigms for DAS is shown in Table 5.

Engineering application

Transportation industry

Civil transportation infrastructure such as railways, highways, tunnels, and embankments have the characteristics of long length, wide distribution range, and long service life. These infrastructures are the lifeline of cities and play an important role in economic and social development. Due to the influence of various factors such as material corrosion, structural aging, and human activities, transportation facilities face potential risks of structural deterioration and damage during their service life [143]. At the same time, the development needs of smart cities have put forward higher requirements for the digitization of transportation infrastructure. Establishing a powerful and efficient monitoring and early warning system is the key to ensuring the safe and reliable operation of infrastructure and preventing long-term potential threats.

For the monitoring and digitalization needs of the transportation field, DAS provides a novel monitoring solution. The large-scale, long-distance, and real-time sensing capabilities of DAS mean that it has irreplaceable advantages in on-site monitoring. In addition, optical cables have strong environmental adaptability and can conveniently collect huge monitoring data along their fiber length.

Rail transit monitoring

In the context of rail transportation, accurate monitoring of train positioning and speed information is crucial to ensure train safety. Traditionally, track circuit technology has been widely used for train positioning and speed monitoring [32]. However, track circuit technology may fail under certain extreme weather conditions. Other sensing technologies also have some application limitations, such as the weak transmission capability of the Global Positioning System (GPS) in tunnels, making it difficult to obtain accurate train motion information. The development of DAS provides a new solution for train positioning and speed monitoring. Since trains generate obvious vibration signals during operation, the sensing optical cable near the train will experience strong vibration, while the sensing optical cable far from the train will record background noise, as illustrated in Fig. 16. Therefore, by analyzing the signal changes at each position of the optical cable, the train's position and running speed can be determined.

In 2014, Peng et al. [33] conducted a field study and laid a sensing cable along the railway track for 10.2 km to record the vibration signals generated by train operation. By analyzing DAS data, the position and running speed of the train at different time points can be clearly observed, which demonstrates the feasibility of DAS in train positioning and speed monitoring. However, using DAS for train positioning and speed monitoring also faces some challenges. For example, how to bury the sensing cable near the track without affecting railway transportation, and how to quickly extract effective information from continuous monitoring data.

Table 5 Summary of Advanced Learning Paradigms

Learning Paradigms	Ref	Year	Preprocessing	Input	Network/ Model	Training dataset	Application scenario (Number of events)
Semi-supervised learning	[126]	2021	Feature extraction	S-T with peak features and energy features	SSAE	Field: 85,920 (labeled) 1,330,315 (unlabeled)	Pipeline safety monitoring (4)
	[125]	2022	wavelet threshold denoising	T	1D-SSGAN	Field: 330 (labeled)	Pavement damage events (3)
	[127]	2022	Denoising	S-T	VGG-16 with FixMatch	Field: 19,017(labeled) 19,359 (unlabeled)	Track defect detection (7)
	[129]	2023	---	MFCC	AlexNet with Valuable data selection	Field: 64 (labeled) 9202 (unlabeled)	Intrusion events (8)
	[128]	2024	---	S-T	MT-ACNN-SA-BiLSTM	Lab: 1230 (labeled) 11,104 (unlabeled)	Perimeter security events (6)
Unsupervised Learning	[131]	2020	Low-pass filter	F	SOM + AE	119	Pipeline safety monitoring
	[132]	2022	---	T	PCA + K-means	2044	blowing vibration events (3)
	[133]	2024	---	T	Transformer	Field: ---	Monitoring offshore wind turbine Cable Protection Systems
Zero-shot learning	[134]	2024	---	S-T	MC-RLGTM	Field: 8277	Disturbance events (7, 1 zero shot event)
	[135]	2024	Band-pass filter	T	APL-ZSL-1DResNet	Field: 500	Intrusion events (2, 1 zero shot event)
Few-shot learning	[58]	2022	---	Mel spectrum with log scale	Cycle-GAN + AlexNet	Field: 3149 2 (few shot type)	Intrusion events (3, 2 few shot events)
	[136]	2024	---	dPhase PSD FBE	Wide ResNet28	Field: 1 and 3 (few shot type)	Cable monitoring (25, 3 few shot events)
Incremental learning	[137]	2023	---	S-T	MTL	Field: 13,329	Cable monitoring (5)
	[138]	2024	VMD denoising	T-F, T	MIFBLS	Field: 4800	Pipeline safety monitoring (4)
	[139]	2024	---	S-T	HECA-ConvNeXt-LwM	Field: 8400	Intrusion events (10)

Table 5 (continued)

Learning Paradigms	Ref	Year	Preprocessing	Input	Network/ Model	Training dataset	Application scenario (Number of events)
Transfer learning	[8]	2021	Band-pass filter	S-T	AlexNet	Field: 1146 (Pretrained on ImageNet)	Intrusion events (8)
	[141]	2022	Band-pass filter	S-T	AlexNet + SVM	Field: 1146 (Pretrained on ImageNet)	Intrusion events (8)
	[140]	2024	Feature extraction	Mel spectrum and Features from T	VGGish-SVM	Lab: 960 (Pretrained on AudioSet)	Perimeter security events (6)

T represents the time domain signal, F represents the frequency spectrum, T-F represents the time–frequency spectrum, and S-T represents the Spatio-temporal image

Field represents data from real-world scenarios, while Lab represents data from laboratory settings

"---" indicates not available

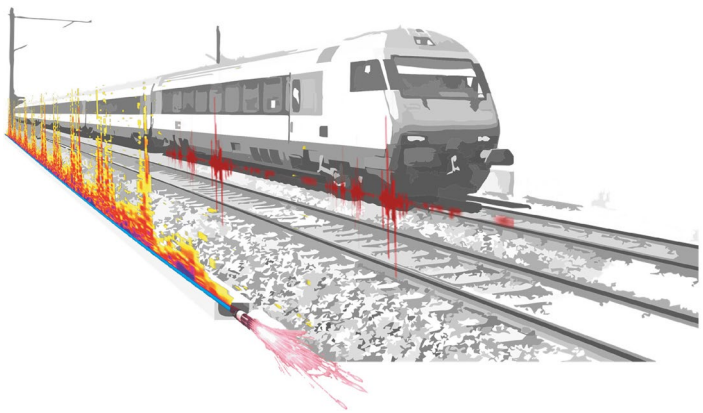

Fig. 16 Schematic diagram of changes in sensing fiber optic cable signals when a train passes [144]

In recent years, various intelligent algorithms have been developed to process sensing data accurately and quickly. Feng et al. [34] proposed an improved Canny algorithm for precise train positioning, and the feasibility of this algorithm has been verified through field experiments, with a positioning error of less than 10 m. The team also proposed a cubic smoothing algorithm with five-point approximation to denoise vibration signals and shorten calculation time. Wiesmeyr et al. [145] proposed a real-time train tracking algorithm based on 1-s signal non-delay operation, which combines machine learning techniques (such as PCA and SVM) with image processing methods (such as edge detection and Kalman filtering). The on-site implementation results show that the accuracy of this real-time tracking algorithm reaches 98%. However, the key issue of accurate positioning of the sensing cable, especially the winding and redundant parts of the cable, is still not perfect. "Tap testing" must be performed to establish the correspondence between the spatial position of the fiber optic cable and the channel number, which takes a considerable amount of time to process. To solve this problem, Vidovic et al. [144]

suggested using train platforms, bridges, and other locations as reference points in engineering practice.

Highway traffic monitoring

If railways are the arteries of a city, connecting different urban clusters to enable regional economic development, then highways are the capillaries of a city, linking thousands of households in the city. The rapid development of smart cities has put forward higher requirements for digital and refined management of highways. In recent years, various monitoring technologies such as road sensors, cameras, and vehicle-mounted GPS have been developed to monitor highway traffic. Although these devices can solve the needs of highway traffic monitoring to a certain extent, they are still inadequate in terms of high-resolution information, maintenance costs, coverage density, data collection frequency, etc., and cannot achieve all-weather high-precision monitoring throughout the region. New traffic monitoring technology is needed, and DAS is a good choice. Compared with railways, the problems encountered in applying DAS to highways are very similar, but due to the randomness of traffic, the signal complexity is higher.

DAS system can provide an alternative solution for highway traffic monitoring. Since the optical cable is buried under the road, this detection method has strong concealment, and the embedded underground optical cable can avoid physical damage during long-term monitoring. In recent years, there have been several good examples of applying DAS to highway traffic monitoring [146–148]. Wang et al. [149] used communication cables under the road to monitor the Pasadena Rose Parade. By analyzing the vibration information collected by the cable, they successfully identified traffic characteristic signals such as pedestrians, motorcycles, and floats. They [150] also proposed a method for measuring road traffic flow and speed to evaluate the impact of sudden events on urban road traffic. By monitoring the ground vibration caused by vehicle movement on the street above the cable through urban telecommunications fiber optic monitoring, the number of vehicles and their average speed can be monitored, proving the feasibility of DAS in highway traffic monitoring. Catalano et al. [151] proposed the application of Hough transform in vehicle counting and demonstrated an algorithm for automatic detection and counting of vehicles. Field tests showed that the accuracy of the algorithm reached 73%. Ye et al. [118] utilized the YOLOv5 framework for real-time vehicle detection in DAS signals and further estimated traffic flow and vehicle speed from DAS data. In traffic detection experiments [150] conducted in the suburbs of Beijing, this method achieved a detection accuracy of 95.9% for passing vehicles, surpassing traditional methods based on inclined stacking. Chiang et al. [152] proposed a deep learning technique to analyze DAS highway traffic signals. This approach employs CNNs to train one-dimensional (1D) DAS time series and two-dimensional (2D) spatiotemporal DAS segments, identifying the correlation between these signals and the weight and other physical characteristics of vehicles, thereby achieving load detection through continuous monitoring. Experimental validation in controlled scenarios demonstrated that this method can achieve 86% vehicle classification accuracy and 94–98% lane occupancy accuracy. Min et al. [153] implemented a series of processing steps to eliminate noise and enhance vehicle signals, generating high-quality labels for subsequent machine learning model training. A total of 190 features (62 one-dimensional and 128 two-dimensional)

extracted from the raw data were reduced to 31 using univariate feature selection, random forest, and similarity analysis. Using the standard SVM machine learning method, these selected features were classified as traffic signals or non-traffic noise. This method achieved an overall accuracy of approximately 80% on the test data. Isolating vehicle signals allows for more accurate estimation of vehicle speed and volume. This study highlights the potential of leveraging existing urban infrastructure for real-time monitoring of traffic flow speed and volume and demonstrates the application prospects of DAS technology in the development of smart cities. To address the challenges of noise pollution and interference from closely traveling vehicles in practical DAS traffic detection applications, Yuan et al. [154] proposed a self-supervised U-Net model. This method suppresses background noise while transforming vehicle-induced DAS signals into high-resolution pulses through spatial deconvolution. Experimental validation under various traffic conditions and driving speeds showed that this method enhances the spatiotemporal resolution of images, improving the distinction of vehicles traveling in close proximity. The spatial deconvolution U-Net model can also analyze large vehicles to identify the number of axles and estimate vehicle length. Monitoring large vehicles is advantageous for imaging deep underground using surface waves induced by vehicle–road dynamic interactions.

In addition to railway and highway monitoring, researchers are also exploring the possibility of more detailed tracking, such as tracking personnel movement. Peng et al. [155] recorded the movement of one person and two people wearing different shoes walking and running at work. Machine learning meets the requirements of human recognition and motion recognition at the same time. The accuracy of supervised machine learning algorithms exceeds 76.25%, and the accuracy of unsupervised machine learning algorithms exceeds 77.65%.

Distributed fiber-optic acoustic sensing technology can meet the application requirements of traffic flow monitoring, road/railway status monitoring, etc. In the transportation field, which helps to improve traffic management efficiency, safety, and urban traffic environment quality. DAS system has shown good potential and feasibility in the monitoring application of the transportation field, providing effective tools for traffic management and planning.

Health monitoring of transportation facilities

The problem of monitoring the health of the track and subgrade structure in railway transportation is also not to be underestimated. Currently, the health monitoring of railway structures mainly relies on manual inspection and conventional track deformation monitoring equipment. However, these methods have a certain monitoring cycle and cannot evaluate the health status of the track in real-time. Commonly used sensors such as accelerometers, strain gauges, and seismic sensing equipment are expensive and cannot be deployed around the track in large numbers for monitoring. DAS has the potential to greatly extend the detection distance with ultra-high sensitivity and can provide an ideal solution for tracking the health monitoring of railway structures. A Field trackside monitoring system is shown in Fig. 17.

In 2019, Kowarik et al. [157] analyzed the data of the ICE 4 train of Deutsche Bahn AG using track views, train views, and bogie cluster data to locate the train signal as well as

the time or spatial direction in the data. This method allows the determination of train speed in three different ways and proposes a new method for train monitoring. In 2020, Christoph et al. [145] proposed a real-time train tracking algorithm. The performance was tested in tunnels with standard cable ducts and open tracks with direct connection cables. This study provides a new idea for train positioning. Guo et al. [156] developed an intelligent detection method for track plate deformation based on a random forest model and conducted on-site experimental verification. The test results show that the intelligent algorithm can effectively identify track plate deformation, and the recognition rate reaches 96.09%. Wang et al. [158] also pointed out that DAS has the potential to detect the health status of the track. They used a deep convolutional network to detect the health status of the track and conducted on-site experiments to verify them. The test results show that the accuracy of the identification method reaches 98.04%. Rahman et al. [159] combined CNN and LSTM models and applied a sliding window for signal enhancement. This approach enabled the monitoring of train positions and the differentiation between normal and abnormal states. Xie et al. [160] proposed a dynamic range extension (RE) phase unwrapping algorithm to recover large amplitude, low SNR signals in DAS systems, eliminating unwrapping errors and enhancing fault tolerance for low SNR signals. Based on this, machine learning algorithms were employed to identify and classify typical track defects, such as transverse RCF, corrugation, and unsupported sleepers, achieving identification accuracy rates exceeding 90%. The above experimental results demonstrate the application potential of DAS in the field of track health monitoring. However, these applications also face some challenges. The trace vibration characteristics that can identify problems may be overwhelmed by strong external noise. In addition, analyzing the health status of the track based on AI technology requires a large amount of annotated data, which is difficult to obtain.

When the train is running at high speed, some of their energy is transmitted in the form of seismic waves due to the compression, friction, and collision between the train

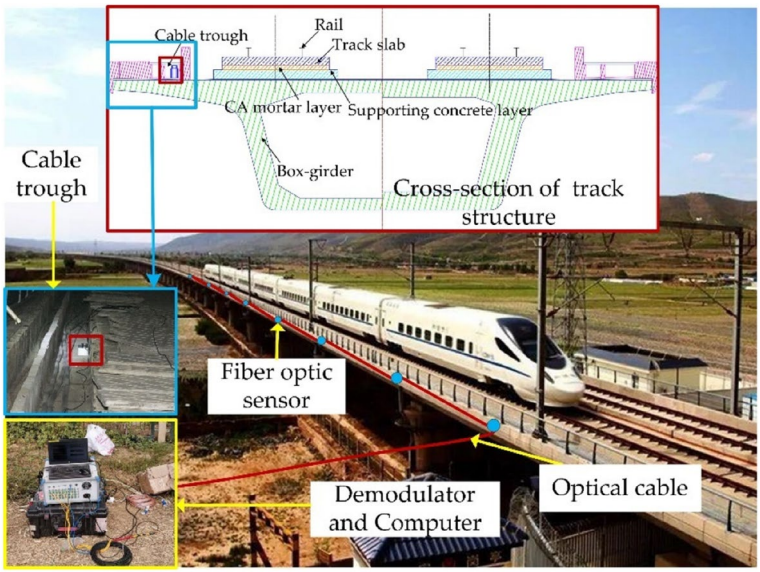

Fig. 17 Field track-side monitoring system [156]

and the track. The seismic waves excited by the train are a good source of active source seismic wave fields, which contain the structural and dynamic characteristics of the track and subgrade [153, 154, 161]. By analyzing the changes of seismic waves, the structural defects of the subgrade can be monitored to achieve disaster warning for high-speed railways. Researchers [162] used DAS to monitor and analyze the seismic signals generated by moving trains. Shao et al. extracted surface wave signals from DAS records using seismic interference technology and then used the multi-analysis surface wave (MASW) method for inversion work. Finally, they successfully obtained the shallow transverse wave velocity structure under the subgrade, fully demonstrating the feasibility of DAS in subgrade velocity structure imaging. Dumont et al. [163] proposed a highly scalable multi-GPU deep learning algorithm, which integrates physical knowledge obtained in the data exploration stage, and then performs deep supervised learning to identify "useful" coherent surface waves generated by human activities. These are a class of seismic waves that are very rich in these records and useful for geophysical imaging. The convolutional residual neural network used was trained on a total of 100,000 labeled images and inferred the coherent surface wave probability map on 170 GB DAS data using 96 CPU cores in 30 min. The application of DAS to analyze seismic waves and obtain the structural status of railway tracks and subgrades is still in its infancy. Trains are mobile sources, and the seismic waves they excite are very complex. DAS is sensitive only to seismic waves propagating in specific directions due to its directional sensitivity, which poses great challenges to the application of DAS in subgrade structure imaging and health monitoring.

Energy industry

Exploration of resources

Predicting underground geological structures has always been a key goal of many geophysical explorations, especially in the oil and gas industry. Estimating the seismic wave velocity and the density of the surrounding medium's structure by measuring ground vibrations on the surface or in boreholes can help predict whether there are potential reservoirs of interest.

DAS was first applied to Shell Canada's CCS project and the US tight gas development project in 2011, which recorded VSP downhole data [35]. Although the quality of DAS measurement data in this study was lower than that of traditional seismic detectors, its simple operation, low cost, and ability to be deployed non-invasively and permanently in a single deployment make it possible to avoid the risk of oil and gas leakage during deployment and to continuously monitor VSP data for a long time after deployment, demonstrating its potential in VSP logging applications. The following year, the same group of researchers [36] improved the response machine used in the experiment, making the DAS measurement data closer to the seismic data measured by traditional seismic detectors. They demonstrated the availability of DAS for typical VSP applications such as lens inspection, imaging, and delay monitoring. They concluded that DAS can be used for VSP monitoring and cost-effective VSP delay monitoring in a variety of wells, including those that traditional seismic detectors cannot detect.

Since then, DAS has been widely used in exploration work in different environments and different types of energy, such as hydrocarbon reservoirs, glaciers, geothermal fields,

salt domes, minerals, and carbon sequestration sites [37–41]. The quality of recorded DAS data can achieve active seismic imaging near the reservoir. Henninges et al. [38] used a hybrid wired fiber optic sensor cable deployed in two 61.4 km deep wells and a new method of DAS to obtain data from three source locations. Accurate time-depth relationships, interval velocities, and corridor stacks were obtained from the recorded data. By comparing the integrated data with data collected from other wells and geological information, it was demonstrated that the DAS method can perform long-term measurements at temperatures up to 150 °C and identify the location of geothermal reservoirs and permeable sandstones, saving a lot of time and cost compared to traditional seismic detector arrays. DAS-VSP was also used for imaging of polymetallic ores. Riedel et al. [42] deployed both systems in boreholes near the target sulfide ore deposit and combined them with active seismic sources in underground tunnels. With this setup, they successfully recorded seismic reflections of the ore deposit and its surrounding geological contrasts, successfully explaining key geological contact points, including the target sulfide mineralization.

Production process monitoring

In production process monitoring, the most widely used DAS technology is in the oil and gas production field. In the development process of oil and gas reservoirs, hydraulic fracturing is required in most cases to transform the reservoir. Timely and accurate downhole information can improve fracturing efficiency, oil well production, and ensure production quality, such as hydraulic fracturing monitoring, oil well integrity testing, microseismic monitoring, and fluid production monitoring. Traditional production monitoring methods such as tracers, flow meters, multiparameter recorders, and fluid scanning imaging instruments have long construction cycles, high monitoring instrument costs, limited distance, production delays, different adaptability to well conditions, difficult installation, and are prone to failure. DAS, with its advantages of low cost, long monitoring time, high resolution sensitivity, and high temperature and pressure resistance, has become an important emerging technology in the production and development of oil and gas reservoirs.

In the monitoring of the fluid process during hydraulic fracturing, Luliia et al. [164] used the acoustic signals measured by DAS to quantitatively explain the distribution of fluids in the fracture cluster based on the correlation between the acoustic signal and the flow rate. They used numerical simulation of the Distributed temperature sensing (DTS) temperature-recovery-inversion model to verify it and obtained MIP-3H well data from Marcelles Laboratory to confirm the feasibility of this method in field tests. The geometric shape of the fracture determines to some extent the degree of increase in production after fracturing. A clear understanding of the geometric shape of the fracture is of great significance for improving performance and optimizing completion design. The application of DAS in strain monitoring can observe the length, height, width, and density of the fracture, which can be used to constrain the geometric shape and model optimization of the fracture. Sherman et al. used a physical thermal–hydraulic-mechanical (THM) model to simulate a series of underground conditions (fracture expansion, fault sliding, etc.) and synthesized DAS measurement results based on the deployment mode of the sensor (horizontal well or vertical well

deployment). They built a database for interested information and trained the initial deep neural network (DNN) through transfer learning combined with the data measured by the on-site DAS equipment. This hybrid data driven DNN model can interpret DAS measurement results almost in real-time. To investigate the mechanism of sound source fluctuations in pipeline leaks and the interaction between distributed fiber optic sensing technology and leakage sound waves, Duan et al. [165] developed a model based on acoustic wave propagation and leakage noise response. They derived the quadratic fitting relationship between pipeline pressure fluctuations and leakage holes, as well as the relationship between the standard deviation of the leakage noise source and the holes. A method [166] for identifying underwater natural gas pipeline leakage signals was proposed, utilizing complete ensemble empirical mode decomposition with adaptive noise (CEEMDAN) permutation entropy and distributed fiber optic acoustic sensing technology. Experimental results validated the theoretical analysis, demonstrating that this method outperforms traditional noise reduction techniques and better preserves the characteristics of the original signal. The RBF neural network model accurately identified four different leakage characteristics, achieving an accuracy of 88.15%. In the imaging problem of hydraulic fracture expansion in unconventional oil and gas reservoirs, the position information of the fiber optic sensor and the DAS measurement value are used as inputs through the trained DNN model to achieve the estimation of the overall range of the fracture. Figure 18 illustrates the structure of the DNN under this scheme.

Security industry

Perimeter security is a key element in safeguarding the lives and property of the people and the political stability of the country. It plays an important role in scenarios such as border lines, fences, pipelines, and maritime monitoring. DAS systems have broad application prospects in the field of perimeter security due to their advantages of wide monitoring range, high concealment, strong environmental adaptability, and no blind spots.

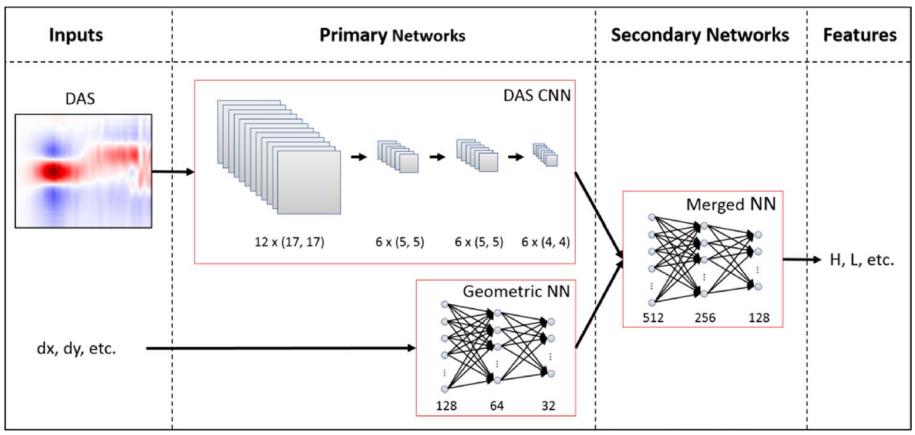

Fig. 18 DNN structure map for crack estimation using DAS measurement data [166]

Intrusion monitoring of surface facilities

The core task of perimeter security on the ground is to monitor the external intrusion from third parties in the security area, quickly detect the type and location of the intrusion event, help management personnel deal with boundary intrusion events, and protect the target from damage. Managers usually face the pressure of long-distance boundary supervision, and traditional methods such as manual inspection cannot achieve real-time monitoring and damage warning in the scene. DAS provides a solution with the ability to locate the occurrence position of events in real-time and report the event type for these scenarios.

In the early application of DAS in perimeter security, the monitored fiber sensing event signals were usually classified manually. The type of event was determined based on the characteristics of the signal in the time–frequency domain, such as waveform, amplitude, phase, etc. Juarez et al. [43] located the intrusion event within 2 km by analyzing the phase changes and waveform differences of the signal when people walked back and forth above the buried optical cable. Mahmoud et al. [44] extracted the horizontal zero-crossing rate feature of the sensing signal and set a threshold and combined with the level crossing (LC) algorithm, to eliminate to some extent the false alarms caused by rainwater interference in the distributed fiber optic security system without affecting the event detection sensitivity.

In the process of exploring the relationship between event signal features and event types, machine learning technology is becoming more and more mature, and cross-disciplinary application research is booming. Some DAS researchers have begun to combine machine learning algorithms to analyze the relationship between intrusion events and signal features.

Shi et al. [9] proposed an event recognition method based on deep learning. This method directly uses the spatiotemporal data matrix of Φ-OTDR as the input of the CNN, and only needs to perform simple bandpass filtering and grayscale transformation as preprocessing to achieve high-accuracy real-time recognition. He et al. [47] proposed an accurate and effective intrusion pattern recognition method based on a two-stage recognition network. In the pre-recognition stage, the decision tree classifier classifies non-intrusion, human-animal activity, and mechanical motion target events based on time energy and frequency spectrum information. In the sub-recognition stage, the target events of human and various animal activities are further distinguished through time–frequency analysis and the combination of BP neural network. This work improves the problem of the increase in the false alarm rate of the intrusion detection system caused by various unknown interferences such as animal activities in complex environments. Barantsov et al. [167] investigated the application of three widely used convolutional neural network architectures—AlexNet, ResNet50, and DenseNet169—in DAS event classification. The AlexNet and DenseNet169 architectures achieved accuracy exceeding 90%. To better identify weak energy intrusion events amidst high-energy background noise, the team [168] proposed a three-channel neural network classifier to separate background noise from event signals. During the processing of DAS spatiotemporal images, two additional images were generated using a denoising autoencoder and an adaptive correlation mathematical model. Wang et al. [101] employed the GASF algorithm to encode external interference signals, transforming one-dimensional time series

signals into more concentrated two-dimensional image features. They then used the ConvNeXt_tiny convolutional neural network model as a classifier. Additionally, transfer learning was utilized to further optimize the network model, resulting in higher classification accuracy and faster convergence. In perimeter security interference recognition experiments involving single-point and multi-point interference, the overall recognition accuracies for six interference events were 99.3% and 98.3%, respectively, with an average recognition time of 0.103 s.

Damage monitoring of buried structures

Typical scenarios for preventing external damage to underground structures include subways, buried optical cables, pipeline monitoring, etc. The construction, maintenance, and repair of underground facilities are usually complex and require special techniques and equipment. Improperly marked or protected underground facilities may become accidental triggers. In addition, facilities such as pipeline cables often involve large-scale energy allocation and transportation, and they often pass through natural environments with extremely complex conditions such as deserts, Gobi, and mountains, facing problems such as difficult inspections, power supply, and monitoring. DAS provides long-distance, high-precision, real-time safety monitoring capabilities for these scenarios, and has the advantages of easy deployment, no power supply, and good scalability, and is widely used in this scenario. Figure 19 illustrates a schematic diagram of a pipeline safety warning system based on DAS.

Tan et al. [170] built an oil and gas pipeline warning system based on SVM, which detects and recognizes different signal features generated under three scenarios of manual excavation, mechanical excavation, and vehicle crossing. The system can identify manual excavation and mechanical excavation events within 5 m of the pipeline and vehicle crossing events within 50 m. However, as the distance between the event occurrence location and the pipeline increases, the event recognition accuracy decreases continuously. Sun et al. [171] treated the event disturbance signals collected in the spatiotemporal domain as images and used image processing technology to preprocess

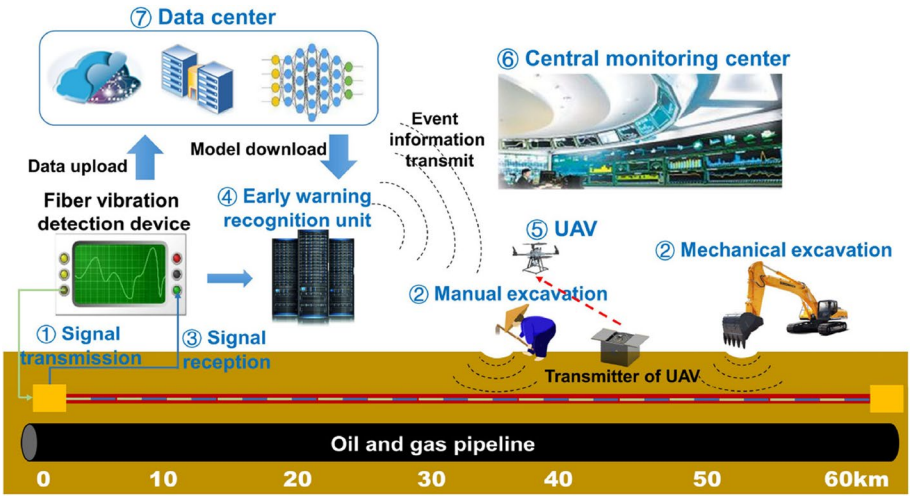

Fig. 19 Schematic diagram of pipeline safety early warning system (UAV: unmanned aerial vehicle) [169]

the images. They selected four highly correlated signal features through image feature extraction and correlation analysis, and then used RVM to determine the event type. The experimental data included waveform signals of three types of events: walking, excavation, and vehicle crossing. The final test results showed that the event recognition accuracy could reach 97.87%, and the recognition time was within 1 s. Wu et al. [27] used a one-dimensional convolutional neural network (1-D CNN) combined with SVM to extract, analyze, and classify event features. They used a multi-scale wavelet decomposition signal-to-noise separation method to improve the SNR of the original data and processed the denoised data using the 1-D CNN + SVM method. Finally, they achieved an average recognition accuracy of more than 98% for the five common events in pipeline safety detection using DAS signals. Ding et al. [172] combined DAS with existing urban underground optical cables, overcame the influence of non-uniformity of underground media in underground pipeline environments through optimization methods such as adaptive short-time energy, fitting optimization based on quality factor, and joint positioning of multiple samples, and achieved precise positioning of vibration sources, providing a monitoring solution for existing underground pipeline intrusion detection without the need for additional construction.

Our research team has developed a city gas pipeline warning system based on our self-developed DAS system, relying on fiber optic cables laid along the pipeline. The system can accurately locate and effectively identify various intrusion events and different interference signals and monitor the safety status of the entire pipeline in real-time. In addition, during the experiment, the system successfully recorded seismic signals that occurred at two different times. The epicenter of these signals was more than 100 km away from the sensing fiber, and the analysis results of P-waves and S-waves were consistent with theoretical expectations. This result shows the huge potential of DAS technology in emergency disaster prevention. The fiber laying path and experimental results are shown in Fig. 20.

Our team [173] has adopted a distributed fiber vibration perception intelligent recognition algorithm that combines a 1-D CNN with a bidirectional long short-term memory neural network (Bi-LSTM). We have successfully achieved accurate identification of destructive warning events such as vehicle loitering, manual destruction, and third-party construction, with a recognition accuracy of over 99.26%. In addition, the team [126] proposed a lightweight distributed fiber AI recognition algorithm based on bilinear convolutional neural network (BCNN) and lightweight gradient boosting machine learning (LightGBM), which can realize event recognition and positioning, and has the ability to deploy distributed fiber real-time warning models at the device edge. To improve the transferability of the fiber warning model, our team [169] also proposed a semi-supervised intrusion event recognition and positioning algorithm based on SSAE, which can improve the recognition accuracy under small sample conditions and achieve low-cost deployment of devices in different regions.

Marine environment perception

To monitor the changes in the ocean environment in real-time, continuous noise monitoring of the ocean is required. Traditional noise monitoring solutions, such as deploying hydrophone arrays on the seabed for real-time noise measurement, can achieve

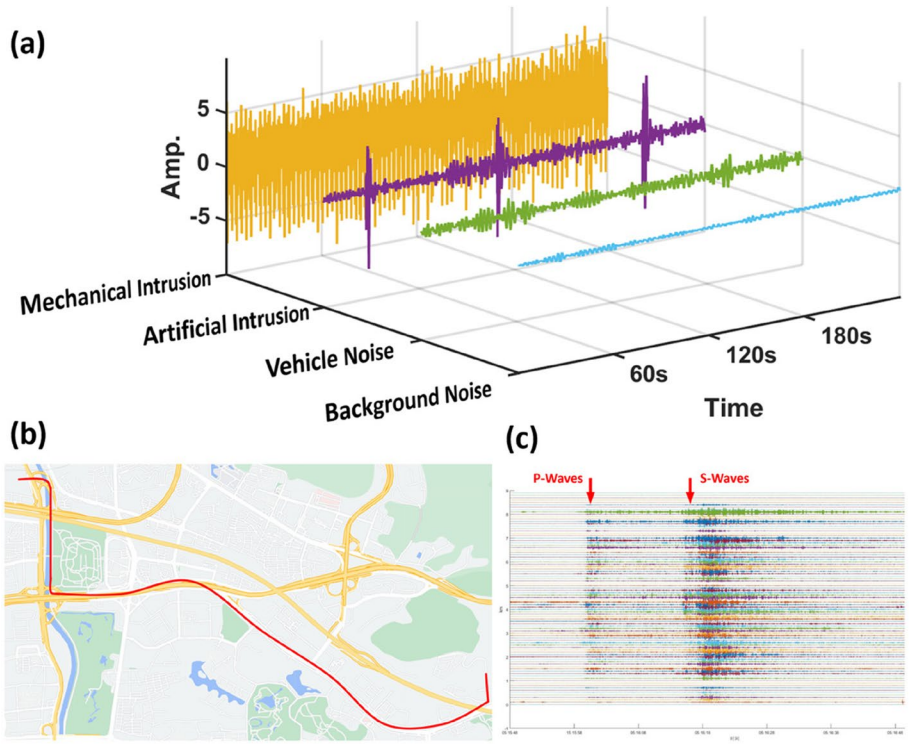

Fig. 20 Pipeline safety warning experiment (**a**) Identification and classification of intrusion and interference signals; **b** Laying lines for gas pipelines; **c** Experimental results of earthquake sensing

real-time monitoring of environmental noise, but the cost of installation and maintenance is high. The application of DAS in the ocean can be combined with existing submarine cables. It only requires the installation of DAS equipment at the submarine cable terminal, which can realize real-time monitoring of ocean environmental noise at much lower cost. Through the collection and processing of ocean environmental noise, seismic waves can be extracted to analyze marine geology, submarine earthquakes, and ocean conditions.

Mateeva et al. [174] analyzed the advantages of DAS VSP compared with traditional VSP, discussed the low-cost and on-demand seismic monitoring of DAS in offshore oil fields, pointed out the huge cost advantage of DAS technology in deep-sea oil field operations, and pointed out the technical development direction of expanding the scope of application. Lindsey et al. [175] combined DAS instruments with existing submarine cables to create a 20 km seismic array with approximately 10,000 components. Based on this seismic array, multiple submarine fault zones were identified, and the sea conditions during the North Pacific storm cycle were tracked based on the amplitude of DAS data collected from microseismic zones. Williams et al. [176] also used DAS technology combined with submarine communication cables to transform submarine cables into seismic sensor arrays, which were used to observe microseismic, local surface gravity waves, and distant seismic waves in the vicinity of Belgium. Magalhaes et al. [177] used chirp pulse DAS (CP-DAS) to obtain more orders of magnitude of submarine seismic data in the seabed environment. They analyzed the data by applying a linear 2D bandpass filter to the frequency-wavenumber representation

of CP-DAS data and compared the data with seismic instrument measurement data in the nearby area. They found that the spectra observed by the two were very similar and had practical significance in seismology and oceanography research. Tonegawa et al. [178] used DAS to observe ocean environmental noise in the submarine cable of the Nankai Trough in Japan, and effectively extracted P-waves and Scholte waves from the noise. They pointed out that it is possible to monitor the seabed structure by extending the observation period. Glubokovskikh et al. [179] found that there is a close relationship between the amplitude of ocean seismic waves measured by DAS and ocean storm climate. They inferred that high-precision monitoring of ocean storms can be achieved by collecting and training sufficient monitoring data. Monitoring sea ice extent is crucial for understanding long-term trends in climate change. Castro et al. [180] applied various machine learning algorithms to identify types of ambient seismic noise in frequency-time spectrogram images. This method utilizes InceptionV3 (a deep CNN) for feature extraction, followed by K-means clustering to identify clusters of similar ambient seismic noise. Using this approach, researchers found evidence of two main types of noise, related to the excitation of ocean gravity waves in open water and the presence of sea ice, with sea ice strong enough to suppress wave action.

In addition to interdisciplinary applications in oceanography and seismology, DAS can also be used to monitor the cable status of offshore wind farms and locate the position information of surface ships in the ocean, as shown in Fig. 21. As offshore wind power expands globally, ensuring the reliable operation of these critical infrastructures is essential.

Ellwood et al. [181] used DAS to monitor the cable status of offshore wind farms. Due to the ability of DAS to collect a large amount of information on physical processes that occur over long linear lengths in real-time, more than 1 TB of data is generated every day. Researchers proposed a method of simplified sampling of DRS data, changing the sampling time interval based on the periodic characteristics of sporadic signals. This method was applied to the export cable of the wind farm and a data

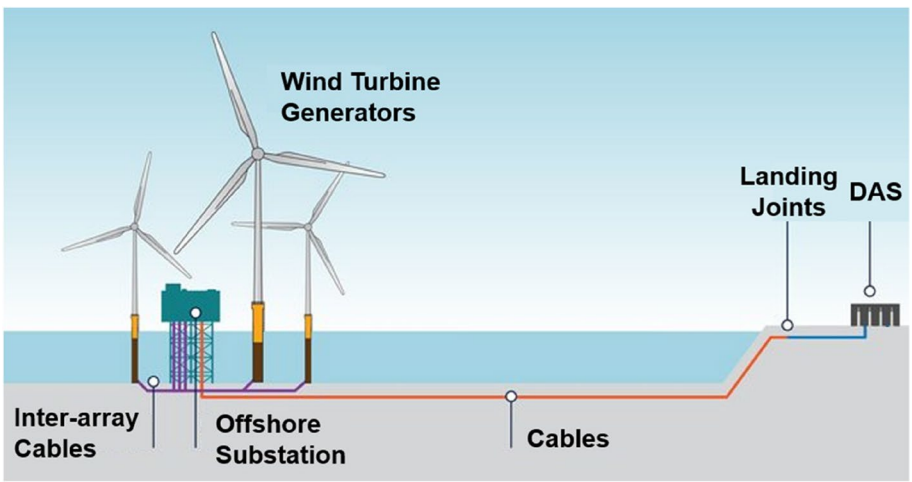

Fig. 21 Deployment diagram of offshore wind farm monitoring equipment

collection experiment lasting 876 h was conducted. The results showed that the data fidelity was sufficient even when less data was collected. Duthé et al. [133] proposed a new unsupervised machine learning method to monitor offshore wind turbine cable protection systems (CPS). This method employs a Transformer neural network to extract high-frequency, noisy DAS time-series signals and uses a contrastive learning scheme to learn coherent data representations. These latent representations can then be used for unsupervised anomaly detection, reducing the need for expensive labeled offshore anomaly data.

Rivet et al. [182] tested the ability to monitor environmental noise and human noise using submarine communication cables with DAS in the Toulon Sea in France. The experiment used a cruise ship to cruise above the cable, and the noise signal collected at a water depth of 85 m and 5.8 km offshore had a high SNR. The ship's radiation noise and other noise were distinguished by spectral analysis, Doppler frequency shift, and other methods. The beamforming analysis can restore the ship's course information. In addition, detection was carried out at a water depth of 2000 m and 20 km offshore, and although the acoustic signal detected was severely attenuated, signals below 50 Hz were still detected. These experiments verified the ability of submarine cables to remotely monitor noise in medium ocean depths. Sun et al. [183] combined the advantages of representation learning, attention mechanisms, and self-supervised learning to propose a Noise Adaptive Masked Autoencoder (NAM-MAE) based intelligent event recognition algorithm, applying it to DAS water boundary security monitoring. This method processes acoustic signals collected by the DAS system, employs unsupervised learning for fading suppression, analyzes spatiotemporal information, extracts unbiased features, and uses these features for supervised classification. In classification experiments involving four typical water boundary security events and five types of field-collected non-anomalous events, NAM-MAE demonstrated superiority over five other related models. Chen et al. [184] proposed an advanced underwater DAS signal processing workflow for DAS data preprocessing, feature extraction, and clustering-based unsupervised event classification. Through experiments with actual submarine communication cables, this method successfully detected and analyzed different seismic activities.

Conclusions and discussions

In this paper, we have reviewed the recent developments of AI-driven DAS technology. Initially, it briefly introduces the fundamental principles of Φ-OTDR-based DAS technology and several demodulation schemes. Subsequently, it elaborates on the application of AI in DAS, covering aspects such as data acquisition and compression, data preprocessing, and machine learning-based event recognition. Following this, we summarize the research on the application of this technology in various industrial fields, including transportation, energy, and security, highlighting its significant potential. Despite the notable advancements in AI + DAS technology in recent years, its broader adoption and application still face numerous challenges and issues:

One major bottleneck is the lack of high-quality datasets. Training AI models requires a large volume of high-quality labeled data, which is time-consuming and costly to obtain and label in the DAS field. While unsupervised and semi-supervised learning can reduce reliance on labeled data, existing AI models still face significant

challenges in these areas, with their performance and stability not yet reaching optimal levels. Additionally, the costs associated with big data processing, particularly in terms of data storage, transmission, and computational resources, cannot be overlooked.

Given the extensive sensing range of DAS, which typically covers diverse scenarios, robustness in complex environments and the generalization ability of models are also key areas of current research. Existing models often exhibit considerable performance fluctuations under different environmental and application conditions. Moreover, current AI models are generally complex and demand significant computational resources, making them difficult to deploy and operate in resource-constrained environments. Developing lightweight and efficient AI models that can be rapidly deployed and operated across various hardware platforms is a crucial direction for future research.

The application of DAS spans multiple disciplines, including engineering, energy, geology, and oceanography. Effectively integrating knowledge from these disciplines to enhance data interpretation capabilities is an important research topic. Additionally, multi-sensor data fusion technology can provide more comprehensive and accurate environmental perception in most scenarios. Effectively integrating and interpreting data from different sensors will further enhance the performance and range of applications of DAS systems.

Future research in this field can be categorized into two main directions. One direction focuses on enhancing DAS performance through AI. Leveraging the powerful learning capabilities of AI, researchers can develop intelligent signal processing technologies, such as AI-based demodulation, sensing RE, and dynamic range enhancement. These technologies can significantly improve DAS system performance, enabling their application in a wider range of scenarios. The other direction involves further research on advanced tasks in various industrial fields. This includes the construction and sharing of large-scale public datasets, optimization of unsupervised training methods, separation and recognition of superimposed signals, development of lightweight models for rapid deployment, and research on robust algorithms for complex situations. These studies will drive the implementation and broader adoption of AI + DAS technology in practical applications.

In conclusion, although AI + DAS technology faces several challenges, its vast application prospects and immense potential make it a field worthy of in-depth research. With the ongoing development and application of AI technology, it is foreseeable that high-performance, intelligent DAS technology will play an indispensable and significant role across various fields, driving rapid industry development.

Acknowledgements
Not applicable.

Authors' contributions
L.S., J.Z., X.C. and D.X. wrote the manuscript with support from H.G., Q.M., F.Y. and S.L. Y.X., H.Z., Y.M., H.L., C.L., and C.Y. provided constructive comments on domain-specific content and participated in the revision of the manuscript. J.Z., X.S., J.S., and Z.H. were responsible for revising the manuscript.

Funding
This work was supported in part by Department of Natural Resources of Guangdong Province, grant number GDNRC [2022] No. 22; Science, Technology and Innovation Commission of Shenzhen Municipality, grant number 20220815121807001; Intelligent Laser Basic Research Laboratory, grant number PCL2021A14-B1. Key Basic Research Scheme of Shenzhen Natural Science Foundation (JCYJ20200109142010888); Hong Kong Research Grants Council(RGC) under General Research Fund 15224521.

Data availability
Data sharing is not applicable to this article as no datasets were generated or analyzed during the current study.

Declarations

Ethics approval and consent to participate
Not applicable.

Consent for publication
Written consent was obtained from all participants for the use of their data and any related materials in this publication.

Competing interests
The authors declare that they have no competing interests.

Received: 30 May 2024 Revised: 8 January 2025 Accepted: 13 January 2025
Published online: 24 February 2025

References

1. Wu H, Zhou B, Zhu K, Shang C, et al. Pattern recognition in distributed fiber-optic acoustic sensor using an intensity and phase stacked convolutional neural network with data augmentation. Opt Express. 2021;29(3):3269–83.
2. Spica ZJ, Ajo-Franklin J, Beroza GC, et al. PubDAS: a public distributed acoustic sensing datasets repository for geosciences. Seismol Res Lett. 2023;94(2A):983–98.
3. Miller DE, Zeng X, Patterson JR, et al. DAS and DTS at Brady Hot Springs: observations about coupling and coupled interpretations. In: 43rd Stanford Workshop on Geothermal Reservoir Engineering. 2018.
4. Cao XM, Su YS, Jin ZY, et al. An open dataset of φ-OTDR events with two classification models as baselines. Results Opt. 2023;10:100372.
5. Yan S, Shang Y, Wang C, et al. Mixed intrusion events recognition based on group convolutional neural networks in DAS system. IEEE Sens J. 2022;22(1):678–84.
6. Yu FH, Shao LY, Liu SQ, et al. Data reduction in phase-sensitive OTDR with ultra-low sampling resolution and undersampling techniques. Sensors. 2022;22(17):6386.
7. Fouda BMT, Yang B, Han D, et al. Pattern recognition of optical fiber vibration signal of the submarine cable for its safety. IEEE Sens J. 2021;21(5):6510–9.
8. Shi Y, Li YH, Zhang YC, et al. An easy access method for event recognition of Φ-OTDR sensing system based on transfer learning. J Lightwave Technol. 2021;39(13):4548–55.
9. Shi Y, Wang YY, Zhao L, et al. An event recognition method for Φ-OTDR sensing system based on deep learning. Sensors. 2019;19(15):3421.
10. Qin ZG, Chen H, Chang J. Detection performance improvement of distributed vibration sensor based on curvelet denoising method. Sensors. 2017;17(6):1380.
11. Qin ZG, Chen H, Chang J. Signal-to-noise ratio enhancement based on empirical mode decomposition in phase-sensitive optical time domain reflectometry systems. Sensors. 2017;17(8):1870.
12. Chen W, Ma XH, Ma QL, et al. Denoising method of the Φ-OTDR system based on EMD-PCC. IEEE Sens J. 2021;21(10):12113–8.
13. Bai YX, Lin TT, Zhong ZC. Noise reduction method of Φ-OTDR system based on EMD-TFPF algorithm. IEEE Sens J. 2021;21(21):24084–9.
14. Zhu T, Xiao XH, He Q, et al. Enhancement of SNR and spatial resolution in φ-OTDR system by using two-dimensional edge detection method. J Lightwave Technol. 2013;31(17):2851–6.
15. He HJ, Shao LY, Li HC, et al. SNR enhancement in phase-sensitive OTDR with adaptive 2-D bilateral filtering algorithm. IEEE Photonics J. 2017;9(3):1–10.
16. Wu MF, Chen YF, Zhu PB, et al. NLM parameter optimization for φ-OTDR signal. J Lightwave Technol. 2022;40(17):6045–51.
17. Li JC, Wang Y, Xiao L, et al. SNR enhancement with a non-local means image-denoising method for a Φ-OTDR system. Appl Opt. 2023;62(9):2283–91.
18. Yu ZH, Zhu L, Dai B, et al. Noise reduction based on adaptive prediction fitting algorithm for a heterodyne Φ-OTDR system. IEEE Photonics Technol Lett. 2022;34(23):1311–4.
19. Wang PF, Lv YJ, Wang Y, et al. Adaptability and anti-noise capacity enhancement for φ-OTDR with deep learning. J Lightwave Technol. 2020;38(23):6699–706.
20. Jiang F, Zhang ZH, Lu ZX, et al. High-fidelity acoustic signal enhancement for phase-OTDR using supervised learning. Opt Express. 2021;29(21):33467–80.
21. Jia HZ, Liang S, Lou SQ, et al. A *k*-nearest neighbor algorithm-based near category support vector machine method for event identification of $\boldsymbol{\varphi}$-OTDR. IEEE Sens J. 2019;19(10):3683–9.
22. Jia HZ, Lou SQ, Liang S, et al. Event identification by F-ELM model for $\boldsymbol{\varphi}$-OTDR fiber-optic distributed disturbance sensor. IEEE Sens J. 2020;20(3):1297–305.
23. Wu HJ, Gan DK, Xu CR, et al. Improved generalization in signal identification with unsupervised spiking neuron networks for fiber-optic distributed acoustic sensor. J Lightwave Technol. 2022;40(9):3072–83.
24. Pan YN, Wen TK, Ye W. Time attention analysis method for vibration pattern recognition of distributed optic fiber sensor. Optik. 2022;251:168127.
25. Lyu CG, Huo ZQ, Cheng X, et al. Distributed optical fiber sensing intrusion pattern recognition based on GAF and CNN. J Lightwave Technol. 2020;38(15):4174–82.

26. Ma YX, Song YC, Song QH, et al. MI-SI based distributed optical fiber sensor for no-blind zone location and pattern recognition. J Lightwave Technol. 2022;40(9):3022–30.
27. Wu HJ, Chen JP, Liu XR, et al. One-dimensional CNN-based intelligent recognition of vibrations in pipeline monitoring with DAS. J Lightwave Technol. 2019;37(17):4359–66.
28. Tejedor J, Macias-Guarasa J, Martins HF, et al. A contextual GMM-HMM smart fiber optic surveillance system for pipeline integrity threat detection. J Lightwave Technol. 2019;37(18):4514–22.
29. Wu HJ, Liu XR, Xiao Y, et al. A dynamic time sequence recognition and knowledge mining method based on the Hidden Markov Models (HMMs) for pipeline safety monitoring with Φ-OTDR[J]. J Lightwave Technol. 2019;37(19):4991–5000.
30. Wu HJ, Yang SQ, Liu XY, et al. Simultaneous extraction of multi-scale structural features and the sequential information with an end-to-end mCNN-HMM combined model for fiber distributed acoustic sensor. J Lightwave Technol. 2021;39(20):6606–16.
31. Zhao X, Sun HB, Lin B, et al. Markov transition fields and deep learning-based event-classification and vibration-frequency measurement for φ-OTDR[J]. IEEE Sens J. 2022;22(4):3348–57.
32. Wybo J-L. Track circuit reliability assessment for preventing railway accidents. Saf Sci. 2018;110:268–75.
33. Peng F, Duan N, Rao Y-J, et al. Real-time position and speed monitoring of trains using phase-sensitive OTDR. IEEE Photonics Technol Lett. 2014;26(20):2055–7.
34. He M, Feng L, Fan J. A method for real-time monitoring of running trains using **Φ**-OTDR and the improved Canny. Optik. 2019;184:356–63.
35. Mestayer J, Cox B, Wills P, et al. Field trials of distributed acoustic sensing for geophysical monitoring [M]. Seg technical program expanded abstracts. Soc Explor Geophys. 2011;2011:4253–7.
36. Mateeva A, Mestayer J, Cox B, et al. Advances in distributed acoustic sensing (DAS) for VSP [M]. SEG Technical Program Expanded Abstracts 2012. Soc Explor Geophys. 2012:1-5.
37. Hall K, Bertram K, Bertram M, et al. Simultaneous accelerometer and optical fibre multi-azimuth walk-away VSP experiment. Newell County: 89th Annual International Meeting, SEG, Expanded Abstracts; 2019. p. 5340–5344, https://doi.org/10.1190/segam2019-3216606.1.
38. Henninges J, Martuganova E, Stiller M, et al. Vertical seismic profiling with distributed acoustic sensing images the Rotliegend geothermal reservoir in the North German Basin down to 4.2 km depth. Solid Earth. 2020.
39. Booth AD, Christoffersen P, Schoonman C, et al. Distributed acoustic sensing of seismic properties in a borehole drilled on a fast-flowing Greenlandic outlet glacier. Geophys Res Lett. 2020;47(13):e2020GL088148.
40. Mateeva A, Lopez J, Chalenski D, et al. 4D DAS VSP as a tool for frequent seismic monitoring in deep water. Lead Edge. 2017;36(12):995–1000.
41. Correa J, Egorov A, Tertyshnikov K, et al. Analysis of signal to noise and directivity characteristics of DAS VSP at near and far offsets—a CO2CRC Otway Project data example. Lead Edge. 2017;36(12):994a1-a7.
42. Riedel M, Cosma C, Enescu N, et al. Underground vertical seismic profiling with conventional and fiber-optic systems for exploration in the Kylylahti Polymetallic Mine, Eastern Finland. Minerals. 2018;8(11):538.
43. Juarez JC, Maier EW, Choi KN, et al. Distributed fiber-optic intrusion sensor system. J Lightwave Technol. 2005;23(6):2081–7.
44. Mahmoud SS, Katsifolis J. Elimination of rain-induced nuisance alarms in distributed fiber optic perimeter intrusion detection systems; proceedings of the Fiber Optic Sensors and Applications VI, 731604, 2009. International Society for Optics and Photonics.
45. Luo K, Wang BW, Guo N, et al. Enhancing SNR by anisotropic diffusion for brillouin distributed optical fiber sensors. J Lightwave Technol. 2020;38(20):5844–52.
46. Abufana SA, Dalveren Y, Aghnaiya A, et al. Variational mode decomposition-based threat classification for fiber optic distributed acoustic sensing. IEEE Access. 2020;8:100152.
47. He T, Sun Q, Zhang S, et al. A dual-stage-recognition network for distributed optical fiber sensing perimeter security system. J Light Technol. 2022;41:4331–40.
48. Milonni PW, Eberly JH. Lasers. New Jersey, USA: Wiley; 1988.
49. Boyd R. Nonlinear optics. Commonwealth of Massachusetts, USA: Academic Press; 2008.
50. Fabelinskii IL. Molecular scattering of light. Berlin, Germany: Springer Science & Business Media; 2012.
51. Izumita H, Koyamada Y, Furukawa S. Stochastic amplitude fluctuation in coherent OTDR and a new technique for its reduction by stimulating synchronous optical frequency hopping. IEEE/OSA J Light Technol. 1997;15(2):267–77.
52. Juarez JC, Maier EW, Choi KN, Taylor HF. Distributed fiber-optic intrusion sensor system. IEEE/OSA J Light Technol. 2005;23(6):2081–7.
53. Wang Z, Zhang L, Wang S, Xue N, Peng F, Fan M, Sun W, Qian X, Rao J, Rao Y. Coherent Φ-OTDR based on I/Q demodulation and homodyne detection. Opt Express. 2016;24(2):853–8.
54. Lu YL, Zhu T, Chen L, Bao X. Distributed vibration sensor based on coherent detection of phase-OTDR. IEEE/OSA J Light Technol. 2010;28(22):3243–9.
55. Masoudi A, Pilgrim JA, Newson TP, et al. Subsea cable condition monitoring with distributed optical fiber vibration sensor. J Light Technol. 2019;37(4):1352–8.
56. Milne D, Masoudi A, Ferro E, et al. An analysis of railway track behaviour based on distributed optical fibre acoustic sensing. Mech Syst Signal Process. 2020;142:106769.
57. Shiloh L, Eyal A, Giryes R, et al. Efficient processing of distributed acoustic sensing data using a deep learning approach. J Light Technol. 2019;37(18):4755–62.
58. Shi Y, Dai SW, Liu XY, et al. Event recognition method based on dual-augmentation for a Φ-OTDR system with a few training samples. Opt Express. 2022;30(17):31232–43.
59. Shang Y, Wang J, Huang S, et al. Fault identification method based on generative adversarial network in distributed acoustic sensing. Meas Sci Technol. 2023;34(11):115117.
60. Westbrook P. Big data on the horizon from a new generation of distributed optical fiber sensors. APL Photonics. 2020;5(2):020401.

61. Stork AL, Baird AF, Horne SA, et al. Application of machine learning to microseismic event detection in distributed acoustic sensing data. Geophysics. 2019;85(5):KS149–60.
62. Wu H, Liu J, Xu J, et al. A comparative study for massive data compression in long-distance distributed optical fiber sensing systems. In: Fifth Asia-Pacific Optical Sensors Conference. Vol. 9655. SPIE; 2015. p. 508-511.
63. Dong B, Popescu A, Tribaldos VR, et al. Real-time and post-hoc compression for data from distributed acoustic sensing. Comput Geosci. 2022;166:105181.
64. Qu S, Chang J, Cong Z, et al. Data compression and SNR enhancement with compressive sensing method in phase-sensitive OTDR. Opt Commun. 2019;433:97–103.
65. Yu FH, Liu S, Shao L, et al. Ultra-low sampling resolution technique for heterodyne phase-OTDR based distributed acoustic sensing. Opt Lett. 2022;47(14):3379–82.
66. Yu F, Liu S, Xu D, et al. Data compression solution for Φ-OTDR: encoding the extracted spectrum. IEEE Sens J. 2024;24(14):22429–38.
67. Wang ZY, Lu B, Ye Q, et al. Recent progress in distributed fiber acoustic sensing with Φ-OTDR. Sensors. 2020;20(22):6594.
68. Li Q, Zhang CX, Li LJ, et al. Localization mechanisms and location methods of the disturbance sensor based on phase-sensitive OTDR. Optik. 2014;125(9):2099–103.
69. Zhang XP, Cao L, Shan YY, et al. Performance optimization for a phase-sensitive optical time-domain reflectometry based on multiscale matched filtering. Opt Eng. 2019;58(5):056114.
70. Li JC, Wang Y, Wang PF, et al. Detection range enhancement for Φ-OTDR using semantic image segmentation. J Light Technol. 2022;40(14):4886–95.
71. Li SC, Liu K, Jiang JF, et al. An ameliorated denoising scheme based on deep learning for Φ-OTDR system With 41-km detection range. IEEE Sens J. 2022;22(20):19666–74.
72. Lapins S, Butcher A, Kendall JM, et al. DAS-N2N: machine learning distributed acoustic sensing (DAS) signal denoising without clean data. Geophys J Int. 2024;236(2):1026–41.
73. Wang H, Lin J, Shao D, et al. Multi-scale interactive network in the application of DAS seismic data processing. Front Earth Sci. 2023;10:991860.
74. Sui J, Zhong Z, Tian Y, et al. Cosine spectral association network for DAS VSP data high-precision recovery. IEEE Trans Geosci Remote Sens. 2024;62:5913313.
75. Wang H, Lin J, Li Y, et al. Self-supervised pre-training transformer for seismic data denoising. IEEE Trans Geosci Remote Sens. 2024;62:5907525.
76. Zhang J, Yan Y, Liu S, et al. Adaptive block-matching and 3D denoising for Φ-OTDR under ultra-low SNR conditions. J Light Technol. 2024;42(13):4698–705.
77. Zhang JM, Yan YY, Liu SQ, et al. Signal-to-noise ratio enhancement of Φ-OTDR based on Block-matching and 3D filtering. In: 2023 Opto-Electronics and Communications Conference (OECC). Shanghai. IEEE; 2023, pp. 1-3.
78. Yao R, Li J, Zhang J, et al. Vibration event recognition using SST-based Φ-OTDR system. Sensors. 2023;23(21):8773.
79. Stajanca P, Chruscicki S, Homann T, et al. Detection of leak-induced pipeline vibrations using fiber—optic distributed acoustic sensing. Sensors. 2018;18(9):2841.
80. Adeel M, Shang C, Hu DY, et al. Impact-based feature extraction utilizing differential signals of phase-sensitive OTDR. J Light Technol. 2020;38(8):2539–46.
81. Shi Y, Chen J, Dai S, et al. Multi-signal feature fusion method with an attention mechanism for the Φ-OTDR event recognition system. Opt Express. 2022;30(23):42086.
82. Huang Y, Cheng S, Li Y, et al. High-efficient disturbance event recognition method of φ -OTDR utilizing region-segmentation differential phase signals. Appl Opt. 2022;61(22):6609.
83. Shi Y, Liu X, Wei C. An event recognition method based on MFCC, superposition algorithm and deep learning for buried distributed optical fiber sensors. Opt Commun. 2022;522:128647.
84. Du X, Jia M, Huang S, et al. Event identification based on sample feature correction algorithm for Φ-OTDR. Meas Sci Technol. 2023;34(8):085120.
85. Huang Y, Zhao H, Zhao X, et al. Pattern recognition using self-reference feature extraction for φ-OTDR. Appl Opt. 2022;61(35):10507.
86. Wang X, Zhang A, Liang S, et al. Event identification of a phase-sensitive OTDR sensing system based on principal component analysis and probabilistic neural network. Infrared Phys Technol. 2021;114:103630.
87. Yi J, Shang Y, Wang C, et al. An intelligent crash recognition method based on 1DResNet-SVM with distributed vibration sensors. Opt Commun. 2023;536:129263.
88. Yang N, Zhao Y, Wang F, et al. Using phase-sensitive optical time domain reflectometers to develop an alignment-free end-to-end multitarget recognition model. Electronics. 2023;12(7):1617.
89. Zhang H, Gao J, Hong B. Φ-OTDR signal identification method based on multimodal fusion. Sensors. 2022;22(22):8795.
90. Wu H, Wang C, Liu X, et al. Intelligent target recognition for distributed acoustic sensors by using both manual and deep features. Appl Opt. 2021;60(23):6878.
91. Wang M, Feng H, Qi D, et al. φ-OTDR pattern recognition based on CNN-LSTM. Optik. 2023;272:170380.
92. Kayan CE, Yuksel Aldogan K, Gumus A. Intensity and phase stacked analysis of a Φ-OTDR system using deep transfer learning and recurrent neural networks. Appl Opt. 2023;62(7):1753.
93. Sun Z, Liu K, Jiang JF, et al. Optical fiber distributed vibration sensing using grayscale image and multi-class deep learning framework for multi-event recognition. IEEE Sens J. 2021;21(17):19112–20.
94. Wang MN, Deng L, Zhong YZ, et al. Rapid response DAS denoising method based on deep learning. J Lightwave Technol. 2021;39(8):2583–93.
95. Sun Q, Li QJ, Chen L, et al. Pattern recognition based on pulse scanning imaging and convolutional neural network for vibrational events in Φ-OTDR. Optik. 2020;219:165205.
96. Saleh NL, Faisal B, Yusri MS, et al. Human activities classification based on φ-OTDR system by utilizing gammatone filter cepstrum coefficient envelope using support vector machine. Opt Laser Technol. 2023;164:109417.

97. Ma BL, Gao RZ, Zhang JJ, et al. A YOLOX-based automatic monitoring approach of broken wires in prestressed concrete cylinder pipe using fiber-optic distributed acoustic. Sensors. 2023;23(4):2090.
98. Hu S, Hu XM, Li JQ, et al. Enhancing vibration detection in Φ-OTDR through image coding and deep learning-driven feature recognition. IEEE Sens J. 2024;24(22):38344–51.
99. Yang Z, Dong H, Zhang F, et al. Distributed optical fiber sensing event recognition based on Markov transition field and knowledge distillation. IEEE Access. 2023;11:19362–72.
100. Wei ZY, Dai ZY, Huang Y, et al. A representation-enhanced vibration signal imaging method based on MTF-NMF for Φ-OTDR recognition. J Light Technol. 2024;42(18):6395–401.
101. Wang YJ, Zhuo W, Liu B, et al. GASF-ConvNeXt-TF algorithm for perimeter security disturbance identification based on distributed optical fiber sensing system. IEEE Internet Things J. 2024;11(10):17712–26.
102. Hua X, Qiu GJ, Karimi HR, et al. TFF-CNN Distributed optical fiber sensing intrusion detection framework based on two-dimensional multi-features. Neurocomputing. 2024;564:126959.
103. Lyu CJ, Jiang JY, Li BH, et al. Abnormal events detection based on RP and inception network using distributed optical fiber perimeter system. Opt Lasers Eng. 2021;137:106377.
104. Chen X, Yang C, Yu H, et al. Research on pattern recognition method for φ-OTDR system based on dendrite net. Electronics. 2023;12(18):3757.
105. Meng H, Wang SL, Gao C, et al. Research on recognition method of railway perimeter intrusions based on Φ-OTDR optical fiber sensing technology. IEEE Sens J. 2021;21(8):9852–9.
106. Tejedor J, Macias-Guarasa J, Martins HF, et al. A hybrid cascade-parallel discriminative-generative model for pipeline integrity threat detection in a smart fiber optic surveillance system. Multimed Tools Appl. 2024.
107. Mi QS, Yu HD, Xiao Q, et al. Intrusion behavior classification method applied in a perimeter security monitoring system. Opt Express. 2021;29(6):8592–605.
108. Li ZQ, Zhang JW, Wang MN, et al. Fiber distributed acoustic sensing using convolutional long short-term memory network: a field test on high-speed railway intrusion detection. Opt Express. 2020;28(3):2925–38.
109. Lyu CG, Huo ZQ, Liu YG, et al. Robust intrusion events recognition methodology for distributed optical fiber sensing perimeter security system. IEEE Trans Instrum Meas. 2021;70(9505109):1–9.
110. Hernández PD, Ramírez JA, Soto MA. Deep-learning-based earthquake detection for fiber-optic distributed acoustic sensing. J Lightwave Technol. 2022;40(8):2639–50.
111. Tian M, Dong H, Cao X, et al. Temporal convolution network with a dual attention mechanism for φ-OTDR event classification. Appl Opt. 2022;61(20):5951.
112. Zhou Z, Jiao WY, Hu X, et al. Open-set event recognition model using 1-D RL-CNN with OpenMax algorithm for distributed optical fiber vibration sensing system. IEEE Sens J. 2023;23(12):12817–27.
113. Wang X, Wang C, Zhang F, et al. Feature fusion-based fiber-optic distributed acoustic sensing signal identification method. Meas Sci Technol. 2023;34(12):125141.
114. Jiao WY, Hu X, Gupta R, et al. Open set intrusion event recognition using anchor point learning for distributed optical fiber system. IEEE Trans Instrum Meas. 2024;73:1–13.
115. Xu WJ, Yu FH, Liu SQ, et al. Real-time multi-class disturbance detection for Φ-OTDR based on YOLO algorithm. Sensors. 2022;22(5):1994.
116. Yang N, Zhao Y, Chen J. Real-time Φ-OTDR vibration event recognition based on image target detection. Sensors. 2022;22(3):1127.
117. Shi Y, Zhang Y, Dai S, et al. Footsteps detection and identification based on distributed optical fiber sensor and double-YOLO model. Opt Express. 2023;31(25):41391–405.
118. Ye Z, Wang W, Wang X, et al. Traffic flow and vehicle speed monitoring with the object detection method from the roadside distributed acoustic sensing array. Front Earth Sci. 2023;10:992571.
119. Wang Y, Zhao S, Wang C, et al. Intelligent detection and recognition of multi-vibration events based on distributed acoustic sensor and improved YOLOv8 model. Opt Fiber Technol. 2024;84:103706.
120. Li SZ, Peng RZ, Liu ZL, et al. Perimeter monitoring of urban buried pipeline threated by construction activities based on distributed fiber optic sensing and real-time object detection. Opt Express. 2024;32(2):2590–606.
121. Abdelli K, Grießer H, Tropschug C, et al. A BiLSTM-CNN based multitask learning approach for fiber fault diagnosis. In: Optical Fiber Communication Conference (OFC) 2021. Washington, DC: Optica Publishing Group; 2021. p. M3C.7.
122. Li YH, Zeng XP, Shi Y. A spatial and temporal signal fusion based intelligent event recognition method for buried fiber distributed sensing system. Opt Laser Technol. 2023;166:109658.
123. Sha Z, Feng H, Rui X, et al. PIG tracking utilizing fiber optic distributed vibration sensor and YOLO. J Light Technol. 2021;39(13):4535–41.
124. Yao RX, Li J, Zhang JR. Research on tiny natural gas leakage monitoring based on HST and YOLO. IEEE Sens J. 2024;24(22):36745–50.
125. He J, Hu X, Zhang D, et al. Semi-supervised learning for optical fiber sensor road intrusion signal detection. Appl Opt. 2022;61(6):C65–72.
126. Yang YY, Zhang HF, Li Y. Long-distance pipeline safety early warning: a distributed optical fiber sensing semi-supervised learning method. IEEE Sens J. 2021;21(17):19453–61.
127. Wang S, Liu F, Liu B. Semi-supervised deep learning in high-speed railway track detection based on distributed fiber acoustic sensing. Sensors. 2022;22(2):413.
128. Li YJ, Cao XM, Ni WH, et al. A deep learning model enabled multi-event recognition for distributed optical fiber sensing. Sci China Inf Sci. 2024;67:132404.
129. Shi Y, Chen JW, Dai SW, et al. Φ-OTDR event recognition system based on valuable data selection. J Lightwave Technol. 2024;42(2):961–9.
130. Almudévar A, Sevillano P, Vicente L, et al. Unsupervised anomaly detection applied to Φ-OTDR. Sensors. 2022;22(17):6515.
131. Peng ZQ, Jian JN, Wen HQ, et al. Distributed fiber sensor and machine learning data analytics for pipeline protection against extrinsic intrusions and intrinsic corrosions. Opt Express. 2020;28(19):27277–92.

132. Zhang J, Zhao X, Zhao Y, et al. Unsupervised learning method for events identification in φ-OTDR. Opt Quant Electron. 2022;54(7):457.
133. Duthé G, L'Homme Y, Abdallah I, et al. Towards unsupervised fault detection for offshore wind turbine cable protection systems using contrastive learning. J Phys. 2024;2767(3):032038 IOP Publishing.
134. Shi Y, Liu HF, Zhang WT, et al. Event recognition method based on feature synthesizing for a zero-shot intelligent distributed optical fiber sensor. Opt Express. 2024;32(5):8321–34.
135. Hu X, Dong HP, Kong Y, et al. Effective zero-shot learning method for event classification in Φ-OTDR sensing systems Φ-OTDR. Opt Express. 2024;32(20):35495–512.
136. Luong HV, Deligiannis N, Wilhelm R, et al. Few-shot classification with meta-learning for urban infrastructure monitoring using distributed acoustic sensing. Sensors. 2024;24(1):49.
137. Wu HJ, Wang YF, Liu XY, et al. Smart fiber-optic Distributed Acoustic Sensing (sDAS) with multitask learning for time-efficient ground listening applications. IEEE Internet Things J. 2024;11(5):8511–25.
138. Zhu CY, Pu YY, Lyu ZL, et al. Multidimensional information fusion and broad learning system-based condition recognition for energy pipeline safety. Knowl Based Syst. 2024;300:112259.
139. Liu ZY, Zhang FX, Sun ZH, et al. Distributed fiber optic sensing signal recognition based on class-incremental learning. Opt Fiber Technol. 2024;87:103940.
140. Gan JQ, Xiao YY, Zhang AD. Fused feature extract method for Φ-OTDR event recognition based on VGGish transfer learning. Appl Opt. 2024;63(20):5411–20.
141. Li Y, Zeng X, Shi Y. Quickly build a high-precision classifier for Φ-OTDR sensing system based on transfer learning and support vector machine. Opt Fiber Technol. 2022;70:102868.
142. Wang X, Zhang G, Lou S, et al. Two-round feature selection combining with LightGBM classifier for disturbance event recognition in phase-sensitive OTDR system. Infrared Phys Technol. 2022;123:104191.
143. Dadfar B, El Naggar MH, Nastev M. Quantifying exposure of linear infrastructures to earthquake-triggered transverse landslides in permafrost thawing slopes. Can Geotech J. 2017;54(7):1002–12.
144. Vidovic I, Marschnig S. Optical fibres for condition monitoring of railway infrastructure—encouraging data source or errant effort? Appl Sci. 2020;10(17):6016.
145. Wiesmeyr C, Litzenberger M, Waser M, et al. Real-time train tracking from distributed acoustic sensing data. Appl Sci. 2020;10(2):448.
146. Liu H, Ma J, Yan W, et al. Traffic flow detection using distributed fiber optic acoustic sensing. IEEE Access. 2018;6:68968–80.
147. Lindsey NJ, Yuan S, Lellouch A, et al. City-scale dark fiber DAS measurements of infrastructure use during the COVID-19 pandemic. Geophys Res Lett. 2020;47(16):e2020GL089931.
148. Chambers K. Using DAS to investigate traffic patterns at Brady Hot Springs, Nevada, USA. Lead Edge. 2020;39(11):819–27.
149. Wang X, Williams EF, Karrenbach M, et al. Rose Parade seismology: Signatures of floats and bands on optical fiber. Seismol Res Lett. 2020;91(4):2395–8.
150. Wang X, Zhan Z, Williams EF, et al. Ground vibrations recorded by fiber-optic cables reveal traffic response to COVID-19 lockdown measures in Pasadena, California. Commun Earth Environ. 2021;2(1):160.
151. Catalano E, Coscetta A, Cerri E, et al. Automatic traffic monitoring by φ-OTDR data and Hough transform in a real-field environment. Appl Opt. 2021;60(13):3579–84.
152. Chiang CY, Zhong R, Jaber M, et al. A distributed acoustic sensor system for intelligent transportation using deep learning. IEEE Internet Things Magaz. 2024;7(5):88–96.
153. Min R, Chen Y, Wang H, et al. DAS vehicle signal extraction using machine learning in urban traffic monitoring. IEEE Trans Geosci Remote Sens. 2024;62:5908510.
154. Yuan S, van Den Ende M, Liu J, et al. Spatial deep deconvolution u-net for traffic analyses with distributed acoustic sensing. IEEE Trans Intell Trans Syst. 2023;25(2):1913–24.
155. Peng Z, Wen H, Jian J, et al. Identifications and classifications of human locomotion using Rayleigh-enhanced distributed fiber acoustic sensors with deep neural networks. Sci Rep. 2020;10(1):21014.
156. Guo G, Cui X, Du B. Random-forest machine learning approach for high-speed railway track slab deformation identification using track-side vibration monitoring. Appl Sci. 2021;11(11):4756.
157. Kowarik S, Hussels M-T, Chruscicki S, et al. Fiber optic train monitoring with distributed acoustic sensing: conventional and neural network data analysis. Sensors. 2020;20(2):450.
158. Wang S, Liu F, Liu B. Research on application of deep convolutional network in high-speed railway track inspection based on distributed fiber acoustic sensing. Opt Commun. 2021;492:126981.
159. Rahman MA, Jamal S, Taheri H. Remote condition monitoring of rail tracks using distributed acoustic sensing (DAS): a deep CNN-LSTM-SW based model. Green Energy Intell Trans. 2024;3(5):100178.
160. Xie L, Li Z, Zhou Y, et al. Railway track online detection based on optical fiber distributed large-range acoustic sensing. IEEE Internet Things J. 2023;11(4):6469–80.
161. Jiang Y, Bao T, Ning J, et al. Spectral characteristics of high-speed rail seismic signal under viaduct. Beijing Da Xue Xue Bao. 2019;55(5):829–38.
162. Shao J, Wang Y, Chen L. Near-surface characterization using high-speed train seismic data recorded by a distributed acoustic sensing array. IEEE Trans Geosci Remote Sens. 2022;60:1–11.
163. Dumont V, Tribaldos V R, Ajo-Franklin J, et al. Deep learning for surface wave identification in distributed acoustic sensing data; proceedings of the 2020 IEEE international conference on big data (big data), Atlanta, GA, USA. IEEE; 2020.
164. Sakaida S, Pakhotina I, Zhu D, et al. Estimation of fracture properties by combining DAS and DTS Measurements; proceedings of the SPE International Hydraulic Fracturing Technology Conference and Exhibition. SPE, Muscat, Oman; 2022.
165. Duan Y, Liang L, Tong X, et al. Application of pipeline leakage detection based on distributed optical fiber acoustic sensor system and convolutional neural network. J Phys D Appl Phys. 2023;57(10):105102.

166. Sherman C, Mellors R, Morris J. Subsurface monitoring via physics-informed deep neural network analysis of DAS; proceedings of the ARMA US Rock Mechanics/Geomechanics Symposium, F. ARMA; 2019.
167. Barantsov IA, Pnev AB, Koshelev KI, et al. Classification of acoustic influences registered with phase-sensitive OTDR using pattern recognition methods. Sensors. 2023;23(2):582.
168. Barantsov IA, Pnev AB, Koshelev KI, et al. Multichannel classifier for recognizing acoustic impacts recorded with a phi-OTDR. Sensors. 2023;23(14):6402.
169. Yang Y, Li Y, Zhang T, et al. Early safety warnings for long-distance pipelines: a distributed optical fiber sensor machine learning approach; proceedings of the Proceedings of the AAAI Conference on Artificial Intelligence; 2021.
170. Tan D, Tian X, Sun W, et al. An oil and gas pipeline pre-warning system based on Φ-OTDR; proceedings of the 23rd International Conference on Optical Fibre Sensors. International Society for Optics and Photonics, Santander, Spain; 2014.
171. Sun Q, Feng H, Yan X, et al. Recognition of a phase-sensitivity OTDR sensing system based on morphologic feature extraction. Sensors. 2015;15(7):15179–97.
172. Ding ZW, Zou NM, Zhang C, et al. Self-optimized vibration localization based on distributed acoustic sensing and existing underground optical cables. J Lightwave Technol. 2022;40(3):844–54.
173. Yang YY, Zhang HF, Li Y. Pipeline safety early warning by multifeature-fusion CNN and LightGBM analysis of signals from distributed optical fiber sensors. IEEE Trans Instrum Meas. 2021;70:1–13.
174. Mateeva A, Lopez J, Mestayer J, et al. Distributed acoustic sensing for reservoir monitoring with VSP. Lead Edge. 2013;32(10):1278–83.
175. Lindsey NJ, Dawe TC, Ajo-Franklin JB. Illuminating seafloor faults and ocean dynamics with dark fiber distributed acoustic sensing. Science. 2019;366(6469):1103–7.
176. Williams EF, Fernandez-Ruiz MR, Magalhaes R, et al. Distributed sensing of microseisms and teleseisms with submarine dark fibers. Nat Commun. 2019;10(1):5778.
177. Magalhaes R, Fernandez-Ruiz M R, Costa L, et al. Underwater seismology using submarine dark fibres. 2020 22nd International Conference on Transparent Optical Networks (ICTON), Bari, Italy. 2020:pp. 1-4.
178. Tonegawa T, Araki E, Matsumoto H, et al. Extraction of p wave from ambient seafloor noise observed by distributed acoustic sensing. Geophys Res Lett. 2022;49(4):e2022GL098162.
179. Glubokovskikh S, Pevzner R, Sidenko E, et al. Downhole distributed acoustic sensing provides insights into the structure of short-period ocean-generated seismic wavefield. J Geophys Res-Sol Ea. 2021;126(12):e2021JB022729.
180. Peña Castro AF, Schmandt B, Baker MG, et al. Tracking local sea ice extent in the Beaufort sea using distributed acoustic sensing and machine learning. Seismic Record. 2023;3(3):200–9.
181. Ellwood R, Godfrey A, Minto C. Initial results from a simplified sub-sampling approach for distributed acoustic sensing. J Phys Conf Ser. 2021;1761:012002.
182. Rivet D, De Cacqueray B, Sladen A, et al. Preliminary assessment of ship detection and trajectory evaluation using distributed acoustic sensing on an optical fiber telecom cable. J Acoust Soc Am. 2021;149(4):2615–27.
183. Sun M, Yu M, Wang H, et al. Intelligent water perimeter security event recognition based on NAM-MAE and distributed optic fiber acoustic sensing system. Opt Express. 2023;31(22):37058–73.
184. Chen S, Han J, Sui Q, et al. Advanced signal processing in distributed acoustic sensors based on submarine cables for seismology applications. J Lightwave Technol. 2023;41(13):4164–75.

Publisher's Note